Novel Connections Between DNA Replication, Telomere Homeostasis, and the DNA Damage Response Revealed by a Genome-Wide Screen for *TEL1/ATM* Interactions in *Saccharomyces cerevisiae*

Brian D. Piening,*,† Dongqing Huang,* and Amanda G. Paulovich*,[1]
*Fred Hutchinson Cancer Research Center, Seattle, Washington 98109, and †Molecular and Cellular Biology Program, University of Washington, Seattle, Washington 98195

ABSTRACT Tel1 is the budding yeast ortholog of the mammalian tumor suppressor and DNA damage response (DDR) kinase ATM. However, *tel1-Δ* cells, unlike *ATM*-deficient cells, do not exhibit sensitivity to DNA-damaging agents, but do display shortened (but stably maintained) telomere lengths. Neither the extent to which Tel1p functions in the DDR nor the mechanism by which Tel1 contributes to telomere metabolism is well understood. To address the first question, we present the results from a comprehensive genome-wide screen for genetic interactions with *tel1-Δ* that cause sensitivity to methyl methanesulfonate (MMS) and/or ionizing radiation, along with follow-up characterizations of the 13 interactions yielded by this screen. Surprisingly, many of the *tel1-Δ* interactions that confer DNA damage sensitivity also exacerbate the short telomere phenotype, suggesting a connection between these two phenomena. Restoration of normal telomere length in the *tel1-Δ xxx-Δ* mutants results in only minor suppression of the DNA damage sensitivity, demonstrating that the sensitivity of these mutants must also involve mechanisms independent of telomere length. In support of a model for increased replication stress in the *tel1-Δ xxx-Δ* mutants, we show that depletion of dNTP pools through pretreatment with hydroxyurea renders *tel1-Δ* cells (but not wild type) MMS-sensitive, demonstrating that, under certain conditions, Tel1p does indeed play a critical role in the DDR.

THE ATM tumor suppressor kinase is a major signaling component of the DNA damage response (DDR) pathway, and patients with homozygous *ATM* mutations are afflicted with the cancer-prone disorder ataxia telangiectasia (AT) (Savitsky *et al.* 1995; Shiloh 2003). *ATM*-deficient cell lines are sensitive to DNA damage, exhibit pronounced checkpoint and double-strand break (DSB) repair defects (Painter and Young 1980; Kastan *et al.* 1992; Kuhne *et al.* 2004), and exhibit significantly reduced phosphorylation levels of DDR targets (Canman *et al.* 1998). Cells from AT patients exhibit accelerated telomere shortening (Metcalfe *et al.* 1996), and ATM is thought to play a role in telomere length regulation through interactions with telomere binding proteins (Wu *et al.* 2007).

doi: 10.1534/genetics.113.149849
Manuscript received September 20, 2012; accepted for publication January 29, 2013
Supporting information is available online at http://www.genetics.org/lookup/suppl/doi:10.1534/genetics.113.149849/-/DC1.
[1]Corresponding author: Fred Hutchinson Cancer Research Center, 1100 Fairview Ave. N., P.O. Box 19024, Seattle, WA 98109-1024. E-mail: apaulovi@fhcrc.org

The *Saccharomyces cerevisiae* ortholog for mammalian *ATM* is *TEL1* (Greenwell *et al.* 1995; Morrow *et al.* 1995; Mallory and Petes 2000). Tel1p is recruited to DSBs via an interaction with the Mre11-Rad50-Xrs2 (MRX; MRN in mammals) DNA-binding complex (Nakada *et al.* 2003), and Tel1 both facilitates efficient end resection through an unknown mechanism and participates in phosphorylation of downstream DDR substrates (Mantiero *et al.* 2007). Following DSB resection, the related kinase Mec1 [ATR in mammals (Cimprich *et al.* 1996)] recognizes RPA-coated, single-strand DNA (ssDNA) at ssDNA–double-strand DNA (dsDNA) junctions via an interaction with Ddc2, and the DNA damage checkpoint is activated (Paciotti *et al.* 2000). The distinct sensing of double-strand and single-strand damaged DNA structures by Tel1p and Mec1p bears a striking resemblance to the different roles of their ATM and ATR counterparts in mammalian cells (Zou and Elledge 2003; Lee and Paull 2007). However, while the loss of *MEC1* results in severe sensitivity to DNA-damaging agents (Weinert *et al.* 1994), Tel1p is not functionally required for checkpoint activation

in response to intrachromosomal DSBs, and the loss of *TEL1* does not significantly sensitize cells to DNA-damaging agents (Greenwell *et al.* 1995; Morrow *et al.* 1995). Despite this, a *mec1 tel1* double mutant is more sensitive to DNA damage than the *mec1* single mutant. These results demonstrate that, although *MEC1* plays the predominant role at intrachromosomal DSBs, *TEL1* does play some role in response to DNA damage in a *mec1* background (Morrow *et al.* 1995).

While Mec1p appears to be the primary responder to DNA damage (with Tel1p functioning in a back-up role), the respective roles of Mec1p and Tel1p are reversed at telomeres. In *S. cerevisiae*, the telomerase enzyme preferentially associates with short telomeres for elongation through an interaction with Cdc13, and this preferential association is dependent on *TEL1* and the MRX complex (Sabourin *et al.* 2007). MRX recruits Tel1p to DNA ends (Fukunaga *et al.* 2011), at which Tel1p phosphorylates one or more substrates to facilitate telomerase recruitment by Cdc13 via an as-yet poorly understood mechanism (Gao *et al.* 2010; Martina *et al.* 2012). *tel1* mutant cells exhibit a decreased frequency of telomere elongation events and decreased telomerase processivity at telomeres (Arneric and Lingner 2007; Chang *et al.* 2007) that leads to progressive telomere shortening (Greenwell *et al.* 1995; Mallory and Petes 2000). Telomeres in *tel1* cells are shortened but are stably maintained; this depends on *MEC1* (Ritchie *et al.* 1999). Telomere erosion in a *mec1 tel1* mutant leads to aneuploidy, senescence, and cell death (Craven *et al.* 2002; Vernon *et al.* 2008; McCulley and Petes 2010). Despite the requirement for *MEC1* in telomere homeostasis in the absence of *TEL1*, Mec1p is not detected at telomeres in wild-type or *tel1-Δ* cells, and the specific role that Mec1p plays in facilitating telomere maintenance in the absence of *TEL1* is not yet understood (McGee *et al.* 2010).

For Tel1p's role in both the DDR and telomere metabolism, significant questions remain. While the kinase was once thought to be functionally redundant with Mec1p in the DDR, recent studies have identified distinct Mec1-independent roles for Tel1p in checkpoint signaling (Mantiero *et al.* 2007), replication fork stability (Doksani *et al.* 2009), and the suppression of genome rearrangements (Lee *et al.* 2008). None of the mechanisms underlying these roles are well understood. At telomeres, the straightforward model consisting of Tel1p phosphorylation of Cdc13 leading to a conformational change that allows for recruitment of the Est1 subunit of telomerase has recently given way to a model of more complex interactions potentially involving multiple kinases, rates of telomere end resection, and other, possibly novel intermediates (Gao *et al.* 2010; Martina *et al.* 2012; Wu *et al.* 2013). Moreover, the mechanism(s) by which MRX and Tel1 are targeted to short telomeres is poorly understood but likely involves constituents of the shelterin complex (Marcand *et al.* 1997; Teixeira *et al.* 2004).

Despite recent characterizations of Mec1-independent roles for Tel1p in the DDR, these roles are apparently either nonessential, infrequently utilized, or redundant with other pathways as the fact remains that the loss of *TEL1* alone does not confer sensitivity to DNA-damaging agents. To comprehensively characterize the contexts by which Tel1p fits into the DNA damage response, we performed genome-wide screens for *TEL1* genetic interactions that cause sensitivity to two different genotoxic agents, methyl methanesulfonate (MMS) and ionizing radiation (IR). From these screens, we have identified a diverse set of mutant backgrounds for which *TEL1* is required for survival upon exposure to DNA damage. We report that, despite the diversity of *tel1-Δ* interactions identified here, most share an additional common phenotype of an exacerbated telomere defect.

Materials and Methods

Media and growth conditions

Yeast-extract-peptone-dextrose (YEPD) and dropout media have been previously described (Paulovich *et al.* 1998). MMS and hydroxyurea (HU) were purchased from Sigma. YEPD and synthetic plates containing MMS were freshly prepared ~15 hr prior to use.

Yeast strains and plasmids

S. cerevisiae strains used in this study are listed in Table 1. Strain BY4741 and the haploid yeast knockout collection were purchased from Open Biosystems. Plasmid p4339 and strain Y7092 were gifts from Charles Boone and Brenda Andrews. Strain SLY60 was a gift from Sang Eun Lee; strain UCC3508 and plasmid pRS313-Y′ were a gift from Daniel Gottschling, and plasmid pVL1107 was a gift from Vicki Lundblad. All gene disruptions were achieved by homologous recombination at their chromosomal loci by standard polymerase chain reaction (PCR)-based methods (Brachmann *et al.* 1998). Briefly, a deletion cassette with a 0.5-kb region flanking the target ORF was amplified by PCR from the corresponding *xxx*::*kanMX* strain of the deletion array (Open Biosystems) and transformed into the target strain for gene knockout. The primers used in the gene disruptions were designed using 20- to 23-bp sequences that are 0.5 kb upstream and downstream of the target gene. A list of primer sequences for all knockouts used in this study is available upon request from the authors.

tel1-Δ double-deletion library construction and screening

The synthetic genetic array (SGA) approach was used to construct a *tel1-Δ* double-deletion library following the protocol described in Tong and Boone (2006). Library replication was performed using floating-pin manual replicators (VP Scientific). For the IR screen, the library was pin-replicated onto fresh YEPD plates and exposed to gamma irradiation using a Mark II ^{137}Cs irradiator (JL Shepherd & Associates) operated at varying dose rates. Plates were analyzed by manual inspection at 24 and 36 hr following IR. For the MMS screen, the library was pin-replicated onto plates

Table 1 *S. cerevisiae* strains

Strain	Genotype	Source
BY4741	*MATa his3Δ1 leu2Δ0 met15Δ0 ura3Δ0*	Open Biosystems
Y7092	MATα *can1Δ::STE2pr-Sp_his5 lyp1Δ his3Δ1 leu2delta0 ura3Δ0 met15Δ0*	Tong and Boone (2006)
UCC3508	*MATa/MATα ura3-52/ura3-52 lys2-801/lys2-801 ade2-101/ade2-101 his3-Δ200/his3-Δ200 trp1-Δ1/TRP1 leu2-Δ1/leu2-Δ1 adh4::URA3-TEL/adh4::URA3-TEL DIA5-1/DIA5-1 ppr1::HIS3/ppr1::LYS2 TLC1/tlc1:LEU2*	Singer *et al*. (1998)
SLY60	*MATΔ3′:intron:ura3Δ5′ hoΔ hmlΔ:ADE1 hmrΔ:ADE1 ade1-100 leu2-3,112 lys5 trp1:hisG ura3Δ3′:intron:HOcs ade3:GAL:HO*	Lee *et al.* (2008)
yBP1020-22	*MATα can1Δ::STE2pr-Sp_his5 lyp1Δ his3Δ1 leu2delta0 ura3Δ0 met15Δ0 tel1::natMX*	This study
yBP1406-08	*MATa his3Δ1 leu2Δ0 met15Δ0 ura3Δ0 hxt3::URA3*	This study
yBP1416-18	*MATΔ3′:intron:ura3Δ5′ hoΔ hmlΔ:ADE1 hmrΔ:ADE1 ade1-100 leu2-3,112 lys5 trp1:hisG ura3Δ3′:intron:HOcs ade3:GAL:HO tel1:natMX*	This study
yBP1423	*MATa his3Δ1 leu2Δ0 met15Δ0 ura3Δ0 hxt3::URA3 tel1::natMX*	This study
yBP1490-91	*MATa his3Δ1 leu2Δ0 met15Δ0 ura3Δ0 hxt3::URA3 pop2::kanMX*	This study
yBP1502-04	*MATa his3Δ1 leu2Δ0 met15Δ0 ura3Δ0 hxt3::URA3 sap30::kanMX*	This study
yBP1505-07	*MATΔ3′:intron:ura3Δ5′ hoΔ hmlΔ:ADE1 hmrΔ:ADE1 ade1-100 leu2-3,112 lys5 trp1:hisG ura3Δ3′:intron:HOcs ade3:GAL:HO tel1::natMX rad17::kanMX*	This study
yBP1508-10	*MATΔ3′:intron:ura3Δ5′ hoΔ hmlΔ:ADE1 hmrΔ:ADE1 ade1-100 leu2-3,112 lys5 trp1:hisG ura3Δ3′:intron:HOcs ade3:GAL:HO tel1::natMX ddc1::kanMX*	This study
yBP1511-13	*MATΔ3′:intron:ura3Δ5′ hoΔ hmlΔ:ADE1 hmrΔ:ADE1 ade1-100 leu2-3,112 lys5 trp1:hisG ura3Δ3′:intron:HOcs ade3:GAL:HO tel1::natMX nup60::kanMX*	This study
yBP1517-19	*MATΔ3′:intron:ura3Δ5′ hoΔ hmlΔ:ADE1 hmrΔ:ADE1 ade1-100 leu2-3,112 lys5 trp1:hisG ura3Δ3′:intron:HOcs ade3:GAL:HO tel1::natMX nup133::kanMX*	This study
yBP1520-21	*MATΔ3′:intron:ura3Δ5′ hoΔ hmlΔ:ADE1 hmrΔ:ADE1 ade1-100 leu2-3,112 lys5 trp1:hisG ura3Δ3′:intron:HOcs ade3:GAL:HO tel1::natMX lsm7::kanMX*	This study
yBP1524-26	*MATΔ3′:intron:ura3Δ5′ hoΔ hmlΔ:ADE1 hmrΔ:ADE1 ade1-100 leu2-3,112 lys5 trp1:hisG ura3Δ3′:intron:HOcs ade3:GAL:HO tel1::natMX sap30::kanMX*	This study
yBP1527-29	*MATΔ3′:intron:ura3Δ5′ hoΔ hmlΔ:ADE1 hmrΔ:ADE1 ade1-100 leu2-3,112 lys5 trp1:hisG ura3Δ3′:intron:HOcs ade3:GAL:HO tel1::natMX hda3::kanMX*	This study
yBP1550-52	*MATa his3Δ1 leu2Δ0 met15Δ0 ura3Δ0 hxt3::URA3 rad17::kanMX*	This study
yBP1553-55	*MATa his3Δ1 leu2Δ0 met15Δ0 ura3Δ0 hxt3::URA3 nup60::kanMX*	This study
yBP1558-60	*MATa his3Δ1 leu2Δ0 met15Δ0 ura3Δ0 hxt3::URA3 tel1::natMX rad17::kanMX*	This study
yBP1564-66	*MATa his3Δ1 leu2Δ0 met15Δ0 ura3Δ0 hxt3::URA3 tel1::natMX nup60::kanMX*	This study
yBP1576-78	*MATa his3Δ1 leu2Δ0 met15Δ0 ura3Δ0 hxt3::URA3 tel1::natMX sap30::kanMX*	This study
yBP1585-87	*MATa his3Δ1 leu2Δ0 met15Δ0 ura3Δ0 hxt3::URA3 tel1::natMX hda3::kanMX*	This study
yBP1608-10	*MATa his3Δ1 leu2Δ0 met15Δ0 ura3Δ0 hxt3::URA3 nup133::kanMX*	This study
yBP1611-13	*MATa his3Δ1 leu2Δ0 met15Δ0 ura3Δ0 hxt3::URA3 tel1::natMX nup133::kanMX*	This study
yBP1622-23	*MATΔ3′:intron:ura3Δ5′ hoΔ hmlΔ:ADE1 hmrΔ:ADE1 ade1-100 leu2-3,112 lys5 trp1:hisG ura3Δ3′:intron:HOcs ade3:GAL:HO tel1::natMX pop2::kanMX*	This study
yBP1630-32	*MATa his3Δ1 leu2Δ0 met15Δ0 ura3Δ0 hxt3::URA3 rad26::kanMX*	This study
yBP1633-35	*MATa his3Δ1 leu2Δ0 met15Δ0 ura3Δ0 hxt3::URA3 tel1::natMX rad26::kanMX*	This study
yBP1636-38	*MATΔ3′:intron:ura3Δ5′ hoΔ hmlΔ:ADE1 hmrΔ:ADE1 ade1-100 leu2-3,112 lys5 trp1:hisG ura3Δ3′:intron:HOcs ade3:GAL:HO tel1::natMX rad26::kanMX*	This study
yBP1669-71	*MATa his3Δ1 leu2Δ0 met15Δ0 ura3Δ0 hxt3::URA3 ccr4::kanMX*	This study
yBP1672-74	*MATa his3Δ1 leu2Δ0 met15Δ0 ura3Δ0 hxt3::URA3 tel1::natMX ccr4::kanMX*	This study
yBP1681-83	*MATa his3Δ1 leu2Δ0 met15Δ0 ura3Δ0 hxt3::URA3 lsm7::kanMX*	This study
yBP1684-86	*MATa his3Δ1 leu2Δ0 met15Δ0 ura3Δ0 hxt3::URA3 tel1::natMX lsm7::kanMX*	This study
yBP1714-16	*MATa his3Δ1 leu2Δ0 met15Δ0 ura3Δ0 hxt3::URA3 hda3::kanMX*	This study
yBP1717-19	*MATa his3Δ1 leu2Δ0 met15Δ0 ura3Δ0 hxt3::URA3 ddc1::kanMX*	This study
yBP1720-22	*MATa his3Δ1 leu2Δ0 met15Δ0 ura3Δ0 hxt3::URA3 tel1::natMX ddc1::kanMX*	This study
yBP1738-40	*MATa his3Δ1 leu2Δ0 met15Δ0 ura3Δ0 hxt3::URA3 tel1::natMX pop2::kanMX*	This study
yBP1787-89	*MATa his3Δ1 leu2Δ0 met15Δ0 ura3Δ0 hxt3::URA3 fyv4::kanMX*	This study
yBP1790-92	*MATa his3Δ1 leu2Δ0 met15Δ0 ura3Δ0 hxt3::URA3 tel1::natMX fyv4::kanMX*	This study
yBP1793-95	*MATa his3Δ1 leu2Δ0 met15Δ0 ura3Δ0 hxt3::URA3 yku80::kanMX*	This study
yBP1796-98	*MATa his3Δ1 leu2Δ0 met15Δ0 ura3Δ0 hxt3::URA3 tel1::natMX yku80::kanMX*	This study
yBP1799-1801	*MATa his3Δ1 leu2Δ0 met15Δ0 ura3Δ0 hxt3::URA3 rad27::kanMX*	This study
yBP1802-04	*MATa his3Δ1 leu2Δ0 met15Δ0 ura3Δ0 hxt3::URA3 tel1::natMX rad27::kanMX*	This study
yBP1805-07	*MATa his3Δ1 leu2Δ0 met15Δ0 ura3Δ0 hxt3::URA3 rad24::kanMX*	This study
yBP1808-10	*MATa his3Δ1 leu2Δ0 met15Δ0 ura3Δ0 hxt3::URA3 tel1::natMX rad24::kanMX*	This study
yBP1838-40	*MATΔ3′:intron:ura3Δ5′ hoΔ hmlΔ:ADE1 hmrΔ:ADE1 ade1-100 leu2-3,112 lys5 trp1:hisG ura3Δ3′:intron:HOcs ade3:GAL:HO tel1::natMX ccr4::kanMX*	This study
yBP1841-43	*MATΔ3′:intron:ura3Δ5′ hoΔ hmlΔ:ADE1 hmrΔ:ADE1 ade1-100 leu2-3,112 lys5 trp1:hisG ura3Δ3′:intron:HOcs ade3:GAL:HO yku80::kanMX*	This study

(continued)

Table 1, *continued*

Strain	Genotype	Source
yBP1844-46	*MATΔ3′:intron:ura3Δ5′ hoΔ hmlΔ::ADE1 hmrΔ::ADE1 ade1-100 leu2-3,112 lys5 trp1:hisG ura3Δ3′:intron:HOcs ade3:GAL:HO tel1::natMX yku80::kanMX*	This study
yBP1847-49	*MATΔ3′:intron:ura3Δ5′ hoΔ hmlΔ::ADE1 hmrΔ::ADE1 ade1-100 leu2-3,112 lys5 trp1:hisG ura3Δ3′:intron:HOcs ade3:GAL:HO rad27::kanMX*	This study
yBP1850-52	*MATΔ3′:intron:ura3Δ5′ hoΔ hmlΔ::ADE1 hmrΔ::ADE1 ade1-100 leu2-3,112 lys5 trp1:hisG ura3Δ3′:intron:HOcs ade3:GAL:HO tel1::natMX rad27::kanMX*	This study
yBP1859-61	*MATΔ3′:intron:ura3Δ5′ hoΔ hmlΔ::ADE1 hmrΔ::ADE1 ade1-100 leu2-3,112 lys5 trp1:hisG ura3Δ3′:intron:HOcs ade3:GAL:HO rad24::kanMX*	This study
yBP1862-64	*MATΔ3′:intron:ura3Δ5′ hoΔ hmlΔ::ADE1 hmrΔ::ADE1 ade1-100 leu2-3,112 lys5 trp1:hisG ura3Δ3′:intron:HOcs ade3:GAL:HO tel1::natMX rad24::kanMX*	This study

containing 0.01% and 0.03% MMS, grown for 2 days at 30°, and analyzed by visual inspection.

MMS/IR spot and colony assays

For serial-dilution spot assays, log-phase cells were serially diluted in PBS and spotted onto YEPD or YEPD + MMS plates using a pin replicator. A subset of the plates was immediately irradiated using the conditions described above. Plates were incubated at 30° and analyzed by visual inspection at 24 and 36 hr.

For colony-based survival assays, three independent transformants were analyzed for each mutant, along with wild-type and *tel1-Δ* controls. Log-phase cells ($\sim 5 \times 10^7$ cells) were sonicated and counted using a Beckman-Dickinson Coulter counter. Cells were serially diluted in PBS and plated onto YEPD or YEPD + MMS plates. For analyzing radiation sensitivity, cells were spread on YEPD plates and the plates were subsequently irradiated as described above. Viability was determined by plating serial dilutions of cultures onto YEPD and scoring the number of colony-forming units (CFU) after 3–4 days at 30°. Viability was calculated as CFU/total cells. For experiments utilizing a low dose rate (0.9 Gy/min), cells were irradiated in 5-ml liquid cultures over a 7.5-hr period prior to plating on YEPD to assess colony-based survival. In experiments in which a HU pretreatment was used, cells were incubated in liquid YEPD media +/− HU (Sigma) at the indicated times. Following the incubation period, cells were washed twice with PBS, counted by Coulter counter, serially diluted, and plated onto YEPD or YEPD + MMS plates.

Gross chromosomal rearrangement and translocation assays

For the measurement of gross chromosomal rearrangement (GCR) frequencies, log-phase cells grown at 30° in YEPD were harvested, sonicated, and counted using a Coulter counter. Cells (1×10^8) were resuspended in 20 ml YEPD and YEPD + 0.003% MMS and grown at 30° overnight. At 15 hr, cells were washed in 5% Na_2SO_3, sonicated, and counted using a Coulter counter. Cells (1×10^9) were plated onto C-Arg-Ser + canavanine + 5-fluororotic acid (FOA) to measure GCR events, and serial dilutions were plated onto YEPD to measure cell viability. GCR plates were incubated for 4–5 days at 30°. Viability was calculated as CFU/total cells, and MMS-induced GCR frequencies were normalized to GCR frequencies from untreated cells.

The *HO*-inducible translocation assay was performed according to Lee *et al.* (2008). Briefly, log-phase cells were sonicated, cell number was determined using a Coulter counter (Beckman Dickinson), and serial dilutions were plated on C-Ura dropout plates containing galactose to induce *HO* expression. Strain growth and translocations in the absence of *HO*-induced DSBs were measured on synthetic complete media and C-Ura plates containing glucose.

Southern blotting

Southern blotting for telomere lengths was carried out using a previously described DNA probe targeting telomeric Y′ regions (Singer *et al.* 1998). DIG-labeled probe synthesis was carried out by PCR using the Roche DIG Probe Synthesis Kit following the manufacturer's instructions. Genomic DNA was prepared using a Yeastar genomic DNA kit (Zymo Research). Genomic DNA preparations were digested overnight with *Xho*I (Invitrogen) and separated on 1% gels. Separated DNA molecules were transferred onto nylon membranes via blot sandwich overnight in 20× SSC buffer. DNA molecules were crosslinked onto the membrane using a UV crosslinker (Fisher Scientific) at 60 mJ/cm^2, and the membrane was incubated with the Y′ telomeric DIG-labeled probe overnight. Antibody detection of the DIG probe was performed using the DIG luminescent detection kit (Roche), and blots were imaged on a ChemiDoc XRS system (Bio-Rad).

Results

Synthetic genetic array screen for interactions with tel1-Δ in response to MMS and IR

To better understand the extent of Tel1p's role in the DDR, we sought to characterize mutant backgrounds in which *TEL1* is required for survival in response to MMS and/or ionizing radiation. To achieve this, we constructed a genome-wide double-deletion library by mating a *MATα tel1-Δ* strain to the *MAT*a haploid deletion library (Winzeler *et al.* 1999) using the SGA procedure developed by Tong *et al.* (2001) and Tong and Boone (2006). The *tel1-Δ xxx-Δ*

double-deletion library was screened for survival on YEPD plates containing either 0.01% or 0.03% MMS. Plates were examined after 24 and 48 hr by visual inspection for double mutants that exhibited MMS sensitivity. Double-mutant strains exhibiting sensitivity were subsequently spotted in 10-fold serial dilutions along with the parental single-mutant strains on YEPD + MMS to confirm the interaction. As an additional verification step, we remade each single and double mutant by PCR-mediated transformation in a new BY4741 parental haploid strain. These new double-deletion mutants were then retested by serial-dilution spot assay on MMS plates and scored by visual inspection. Interactions passing this second criterion were then subjected to colony survival analyses to quantify the degree of interaction with *tel1-Δ* on MMS plates. After validation, 13 gene deletions showed enhanced sensitivity to MMS when paired with *tel1-Δ* (Figure 1A). These genes include multiple subunits of the 9-1-1 checkpoint clamp (*RAD17*, *DDC1*; ~400-fold) as well as the 9-1-1 clamp loader *RAD24* (deletion of the third subunit *mec3-Δ* grows poorly in BY4741 and could not be evaluated in the SGA screen) and members of the CCR4-NOT deadenylase complex (*CCR4* and *POP2*; 6- to 130-fold). Additional interactions exhibiting >10-fold increases in MMS sensitivity were between *TEL1* and the base excision repair endonuclease *RAD27* (~30-fold) and the histone deacetylase (HDAC) subunit *HDA3* (~30-fold). Additional genes exhibiting <10-fold interactions with *tel1-Δ* consisted of two nucleoporins (*NUP60* and *NUP133*), the nonhomologous end-joining (NHEJ) repair factor *YKU80*, a second HDAC subunit (*SAP30*), the *RAD26* ATPase, and a member of the Sm-like mRNA decay family (*LSM7*). We note that, in the initial and confirmative screens, an additional *tel1-Δ* interaction with the uncharacterized *FYV4* gene exhibited a growth defect with *tel1-Δ* as well as a >10-fold increase in MMS sensitivity. However, the *FYV4* ORF is located ~200 bp upstream of the transcription start site of the essential mediator subunit *MED6*. Transforming the *fyv4-Δ tel1-Δ* strain with a plasmid containing the *MED6* gene and its promoter completely abolished the growth defect and MMS sensitivity of this strain (data not shown), leading us to conclude that the *fyv4-Δ* gene replacement exerts an off-target effect on the essential *MED6* gene. Due to these complications, the *FYV4/MED6* candidate was removed from further consideration in this study.

As our MMS screen revealed a diverse set of interactions that cause enhanced MMS sensitivity with *tel1-Δ*, we asked whether a different set of mutants would interact with *tel1-Δ* in response to a different DNA-damaging agent, γ-irradiation. To test for genetic interactions with *tel1-Δ* in ionizing radiation, the *tel1-Δ xxx-Δ* double-deletion library was plated onto YEPD and exposed to either 200 or 400 Gy of ionizing radiation. In contrast to the MMS screen, only the 9-1-1 checkpoint genes *rad17-Δ*, *ddc1-Δ*, and *rad24-Δ* exhibited interactions with *tel1-Δ* in response to IR, and these interactions were minor (<10-fold) in comparison to the *9-1-1-Δ tel1-Δ* interactions in MMS (>100-fold) (Figure 1B). To confirm that the *tel1-Δ xxx-Δ* interactions identified in the MMS sensitivity screen were indeed not also sensitive to IR, we tested each of the 13 MMS-sensitive *tel1-Δ xxx-Δ* strains for IR sensitivity. Consistent with the screen results, only the *9-1-1-Δ tel1-Δ* double mutants exhibited enhanced IR sensitivity (Figure 1B).

As MMS is often referred to as a "radiomimetic" agent, the finding that many of the MMS interactions were not recapitulated using IR was unexpected. One possible explanation for this is that the 400 Gy of IR was delivered as a pulse over a short period of time (8 Gy/min), while for MMS treatment cells were grown continuously in 0.03% MMS. [DNA damage phenotypes can differ significantly when the agent is delivered as a pulse or chronic treatment (Murakami-Sekimata *et al.* 2010).] To test this hypothesis, three of the *tel1-Δ xxx-Δ* double mutants identified in our screen (*ccr4-Δ tel1-Δ*, *hda3-Δ tel1-Δ*, and *rad17-Δ tel1-Δ*) were examined for sensitivity to the same 400-Gy cumulative dose of IR (as in Figure 1B), but this time delivered chronically over a period of 7.5 hr (0.9 Gy/min). As seen in Figure 1C, the total IR sensitivity for wild-type and single-mutant strains was increased somewhat in the chronic exposure relative to the pulse of 400 Gy (Figure 1B); however, no additional (*i.e.*, aside from 9-1-1) interactions with *tel1-Δ* were observed, and the *rad17-Δ tel1-Δ* interaction was reduced. From this, we conclude that, unlike the MMS case, *tel1-Δ* interactions in IR are limited to mutations in the 9-1-1 pathway.

Loss of telomerase is associated with a progressive increase in MMS sensitivity

Mammalian cells with shortened telomeres exhibit increased sensitivity to DNA-damaging agents via an as-yet-unknown mechanism (Goytisolo *et al.* 2000; Wong *et al.* 2000; Gonzalez-Suarez *et al.* 2003; Nakamura *et al.* 2005; Agarwal *et al.* 2008; Soler *et al.* 2009; Drissi *et al.* 2011; Woo *et al.* 2012). Based on this precedent, we hypothesized that resistance to DNA-damaging agents in yeast would also be tightly linked to telomere length and that yeast cells would become more sensitive to DNA damage in a progressive manner as telomeres shorten. To evaluate this possibility, we employed a heterozygous diploid *tlc1* strain, which, upon sporulation into haploid progeny, exhibits progressive telomere shortening that leads to eventual replicative senescence (Singer and Gottschling 1994). After inducing sporulation, we subcultured *TLC1* and *tlc1* haploid progeny over a series of days, and each day we removed an aliquot of cells for testing of survival on YEPD or YEPD + MMS plates. In the absence of MMS, *tlc1* strains exhibited progressive telomere shortening over the 3-day period, while telomere lengths in the *TLC1* strains remained unchanged over the same period (data not shown). When tested for viability on plates containing either 0.01% or 0.03% MMS, *TLC1* strains showed minimal MMS sensitivity that was unchanged over the course of the experiment (Figure 2). In contrast, the *tlc1* mutant strains exhibited a progressive and dose-dependent

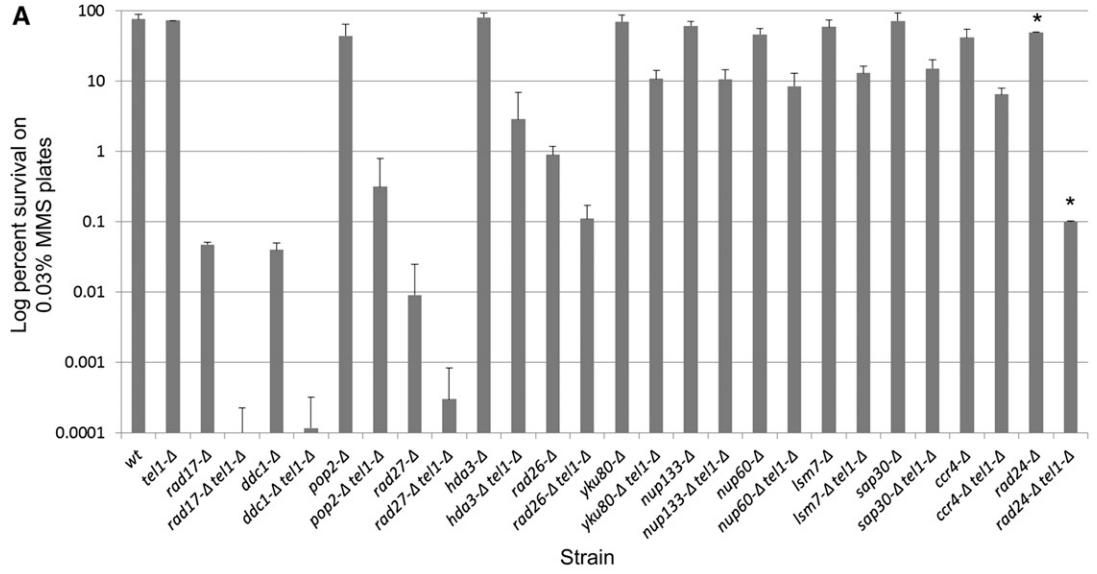
A
Log percent survival on 0.03% MMS plates
100
10
1
0.1
0.01
0.001
0.0001
*
*
wt
tel1-Δ
rad17-Δ
rad17-Δ tel1-Δ
ddc1-Δ
ddc1-Δ tel1-Δ
pop2-Δ
pop2-Δ tel1-Δ
rad27-Δ
rad27-Δ tel1-Δ
hda3-Δ
hda3-Δ tel1-Δ
rad26-Δ
rad26-Δ tel1-Δ
yku80-Δ
yku80-Δ tel1-Δ
nup133-Δ
nup133-Δ tel1-Δ
nup60-Δ
nup60-Δ tel1-Δ
lsm7-Δ
lsm7-Δ tel1-Δ
sap30-Δ
sap30-Δ tel1-Δ
ccr4-Δ
ccr4-Δ tel1-Δ
rad24-Δ
rad24-Δ tel1-Δ
Strain

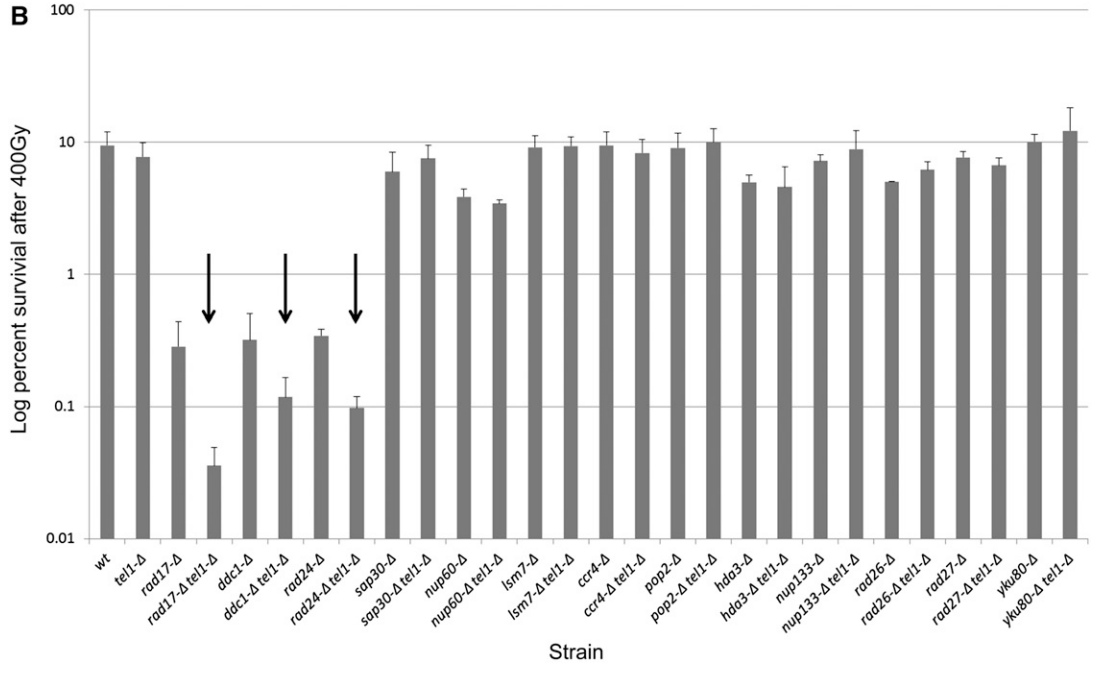
B
Log percent survivial after 400Gy
100
10
1
0.1
0.01
wt
tel1-Δ
rad17-Δ
rad17-Δ tel1-Δ
ddc1-Δ
ddc1-Δ tel1-Δ
rad24-Δ
rad24-Δ tel1-Δ
sap30-Δ
sap30-Δ tel1-Δ
nup60-Δ
nup60-Δ tel1-Δ
lsm7-Δ
lsm7-Δ tel1-Δ
ccr4-Δ
ccr4-Δ tel1-Δ
pop2-Δ
pop2-Δ tel1-Δ
hda3-Δ
hda3-Δ tel1-Δ
nup133-Δ
nup133-Δ tel1-Δ
rad26-Δ
rad26-Δ tel1-Δ
rad27-Δ
rad27-Δ tel1-Δ
yku80-Δ
yku80-Δ tel1-Δ
Strain

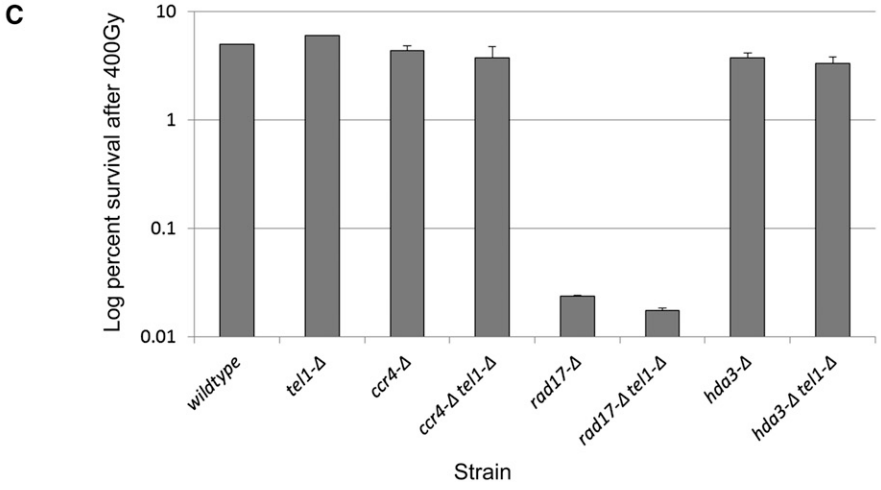
C
Log percent survival after 400Gy
10
1
0.1
0.01
wildtype
tel1-Δ
ccr4-Δ
ccr4-Δ tel1-Δ
rad17-Δ
rad17-Δ tel1-Δ
hda3-Δ
hda3-Δ tel1-Δ
Strain

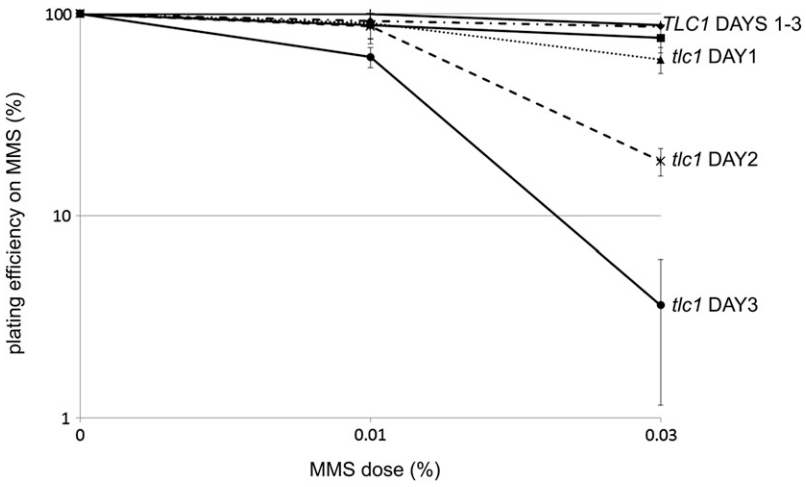

Figure 2 Telomerase-null cells exhibit a progressive increase in MMS sensitivity. *TLC1* and *tlc1* haploid spores from freshly dissected tetrads were subcultured in YEPD over multiple days. Each day, an aliquot was removed and assayed for MMS sensitivity by colony-forming assay. Error bars represent the standard deviation of values from three independent spores.

increase in MMS sensitivity that was most pronounced by day 3 on 0.03% MMS plates (survival rates in MMS were normalized to rates on YEPD alone to correct for MMS-independent loss of viability). As the half-life of telomerase RNA is a few hours (Chapon *et al.* 1997) and the MMS sensitivity manifests after *days*, we conclude that MMS sensitivity is telomere length-dependent in *tlc1* cells, rather than due to *TLC1* loss alone. These results raised the interesting possibility that the DNA damage sensitivity exhibited by the identified *tel1-Δ xxx-Δ* interactions results from an exacerbation of the well-known telomere length defect caused by loss of *TEL1*.

Many of the tel1-Δ MMS interactions exhibit shortened telomeres

As cellular sensitivity to MMS increases progressively with telomere shortening (Figure 2), we hypothesized that some or all of the interactions identified in the *tel1-Δ* screen exacerbate the *tel1*-mediated telomere length defect and that this may be a cause for DNA damage sensitivity in these cells. Thus we asked whether any of the *tel1-Δ xxx-Δ* double mutants exhibited telomere lengths that were significantly shorter than either corresponding single mutant. To answer this question, we isolated genomic DNA from single and double mutants for each of the 13 *tel1-Δ xxx-Δ* interactions and analyzed *Xho*I fragments by Southern blotting with a Y′ subtelomeric probe (Singer *et al.* 1998). As expected (Lustig and Petes 1986; Greenwell *et al.* 1995; Morrow *et al.* 1995), the *tel1-Δ* single mutant exhibited shorter telomere lengths relative to a wild-type strain (Figure 3). Additionally, a number of the other single mutants exhibited shorter telomere lengths relative to the wild type, including *yku80-Δ*, *rad27-Δ*, and *sap30-Δ*, with the *yku80-Δ* mutant being the only single mutant exhibiting a shorter telomere length than *tel1-Δ* (Figure 3). Notably, the 9-1-1 mutants *ddc1-Δ* and *rad17-Δ* were shown in a previous study to exhibit a minor telomere defect (Longhese *et al.* 2000). However, we did not observe discernible shortening of these mutants relative to the wild type (Figures 3 and 4); this may reflect differences in the strain background used in these studies. Notably, the *9-1-1-Δ tel1-Δ* double mutants (*rad24-Δ tel1-Δ*, *rad17-Δ tel1*, and *ddc1-Δ tel1-Δ*) exhibited very short telomeres relative to *tel1-Δ*, and a second class consisting of *sap30-Δ tel1-Δ*, *ccr4-Δ tel1-Δ*, *pop2-Δ tel1-Δ*, *hda3-Δ tel1-Δ*, *nup133-Δ tel1-Δ*, *nup60-Δ tel1-Δ*, *rad27-Δ tel1-Δ*, and *yku80-Δ tel1-Δ* also exhibited shorter telomeres relative to *tel1-Δ*. The *rad26-Δ tel1-Δ* and *lsm7-Δ tel1-Δ* double mutants exhibited telomere lengths that were identical to *tel1-Δ*. Our finding that 11 of the 13 *tel1-Δ xxx-Δ* interactions exhibited decreased telomere lengths relative to *tel1-Δ* is unexpected, since many of identified genes play no known role in telomere metabolism. To exclude the possibility that the *tel1-Δ xxx-Δ* short telomere phenotype was not merely an artifact due to a previously characterized phenotypic lag for *tel1* telomeres

Figure 1 Quantitative survival analysis for *tel1* interactions in MMS and IR via colony-forming assay. (A) Quantitative survival analysis in MMS. Log-phase cultures for three independent transformants of each single and double mutant were serially diluted in PBS and spread onto YEPD or YEPD + 0.03% MMS plates (asterisks indicate that screening was done in 0.015% MMS due to extreme MMS sensitivity). Viable cells were determined by the number of CFU after 3 days at 30°. (B) Quantitative survival analysis in IR. Log-phase cultures for three independent transformants of each single and double mutant were serially diluted in PBS and spread onto YEPD plates and irradiated at 400 Gy at 8 Gy/min. Viable cells were determined by the number of CFU after 3 days at 30°. Arrows indicate interactions identified in the genome-wide screen. Error bars represent the standard deviation of values from three independent transformants. (C) Quantitative survival analysis using continuous low-dose-rate IR. Log-phase cultures for two independent transformants of each single and double mutant were diluted in YEPD in 15-ml tubes and irradiated with 400 Gy delivered at a continuous dose rate of 0.9 Gy/min over 7.5 hr. Following delivery of IR, cells were counted, serially diluted, and plated for colony survival analysis. Error bars show the range of values for two independent transformants.

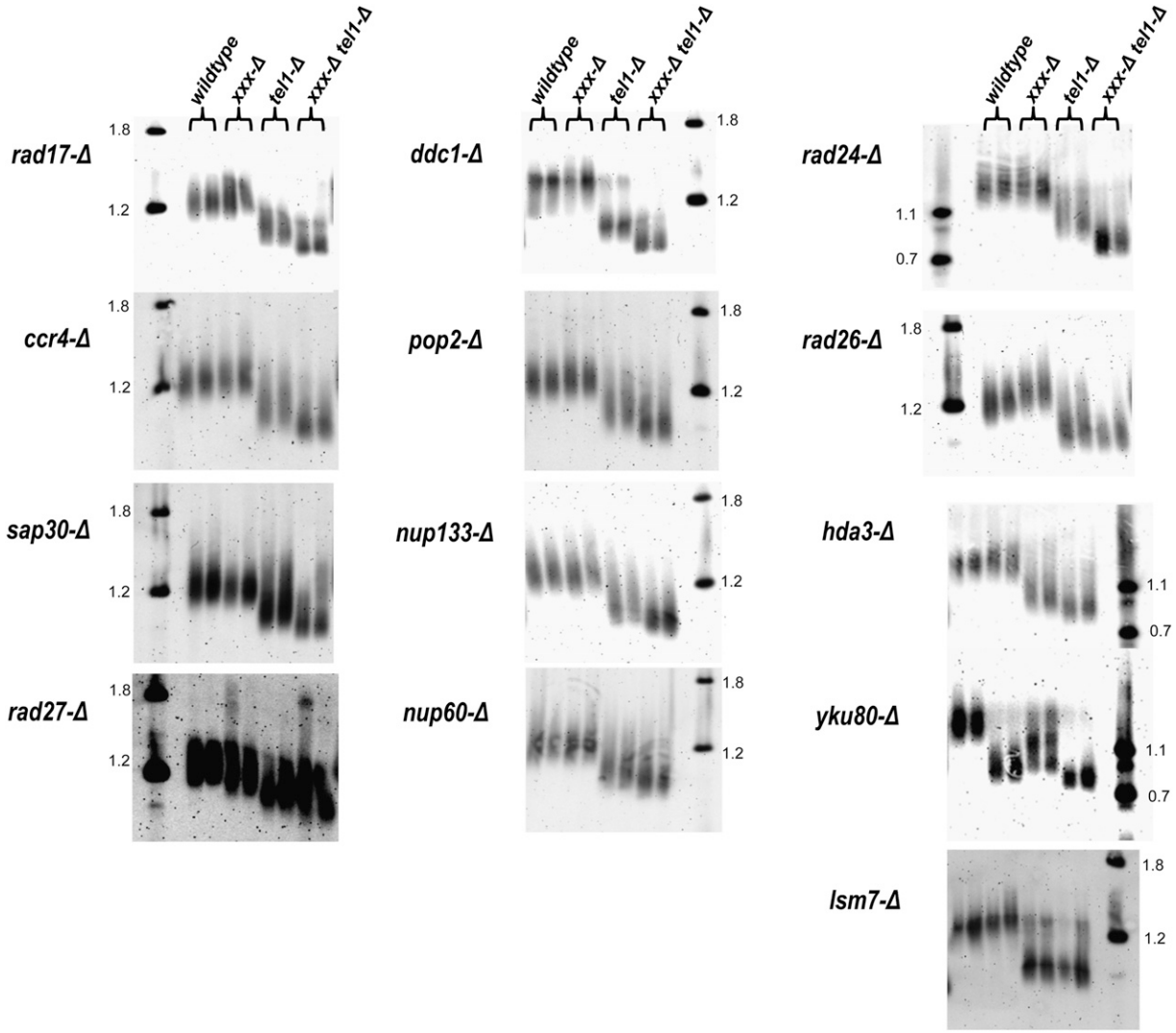

Figure 3 Telomere lengths for *tel1*-Δ MMS-sensitive interactions. For each strain, *Xho*I-digested DNA was analyzed by Southern blot using a probe complementary to the Y′ subtelomere. Each *xxx-Δ* mutant is listed to the left of each corresponding blot, and duplicates representing independent transformants for each strain are loaded side by side (duplicates are indicated by the brackets above). DNA ladders (in kb) are indicated in the far left or right lane of each blot.

[∼150 generations (Lustig and Petes 1986)], we examined telomere lengths for a selection of single and double mutants over additional subculturing for a period of 5 days. During the repeated subculturing, we did not observe any further changes in telomere length by Southern blot (Figure 4). From these data, we conclude that the majority of *tel1-Δ* interactions identified in the MMS sensitivity screen also confer shorter telomeres, suggesting a possible connection between the two phenotypes.

Artificial elongation of telomeres in tel1-Δ 9-1-1-Δ mutants partially suppresses MMS sensitivity

As telomere shortening was shown to be causative for MMS sensitivity in the *tlc1* case (Figure 2), we next hypothesized that the exacerbated telomere defect exhibited by the majority of *tel1-Δ xxx-Δ* strains (Figure 3) may be causative for enhanced MMS sensitivity. Thus, reversal of the telomere length defect would also reduce the MMS sensitivity of these mutants. To test this, we transformed each of the *tel1-Δ xxx-Δ* single and double mutants with a plasmid expressing a fusion of the Cdc13 capping protein to the Est2 subunit of telomerase (Evans and Lundblad 1999). This fusion has been previously shown to alleviate the short telomere phenotype in a *tel1* mutant (Tsukamoto *et al.* 2001). A panel of *tel1-Δ xxx-Δ* mutant strains with and without the *CDC13-EST2* plasmid was screened for sensitivity by spotting cells on MMS plates (supporting information, Figure S1). Of the tested *tel1-Δ xxx-Δ* interactions, the *rad24-Δ tel1-Δ* strain exhibited a visible increase in survival on MMS plates when transformed with the *CDC13-EST2* fusion plasmid (and not the vector). None of the other *tel1-Δ xxx-Δ* interactions exhibited any change in MMS sensitivity upon transformation with *CDC13-EST2*. We confirmed the suppression of MMS sensitivity in *rad24-Δ tel1-Δ* as well as a second 9-1-1

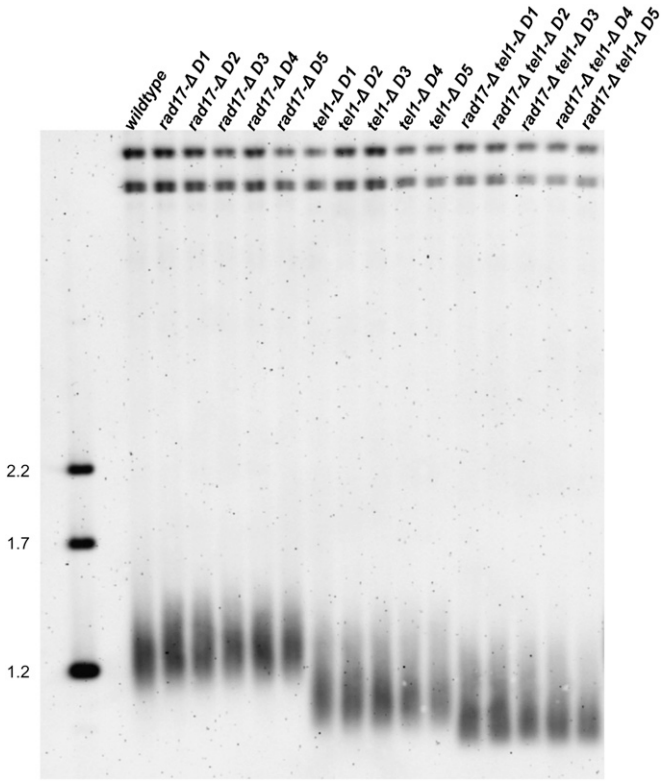

Figure 4 Repeated subculturing does not alter telomere lengths. Wild-type, *tel1-Δ*, *rad17-Δ*, and *rad17-Δ tel1-Δ* cultures were diluted in fresh YEPD media and grown overnight. Genomic DNA was harvested the following day, and a portion of the cells was diluted in fresh medium and cultured overnight. The process was repeated over a period of 5 days (D1–D5). *Xho*I-digested DNA was analyzed by gel electrophoresis and Southern blotting with a probe recognizing subtelomeric Y′ sequence. Molecular weight markers are indicated on the left (in kb).

component (*rad17-Δ tel1-*Δ) by a quantitative colony-forming assay (Figure 5, A and B), and again the fusion plasmid conferred discernible (but not total) resistance to MMS (11-fold for *rad24-Δ tel1-Δ* and 4-fold for *rad17-Δ tel1-Δ vs.* the vector). Telomeres in these strains were significantly elongated to wild-type levels by addition of the *CDC13-EST2* fusion and were hyper-elongated in wild-type and *tel1-Δ* strains (Figure 5C). (*CDC13-EST2* was able to elongate telomeres to an identical degree in other non-9-1-1-related *tel1-Δ xxx-Δ* interactions (not shown) despite having no effect on MMS resistance.) While expression of *CDC13-EST2* suppresses strong (>100-fold) MMS sensitivity in *9-1-1-Δ tel1-Δ* interactions by ~10-fold (Figure 5), the fact that this suppression is not total and that *CDC13-EST2* expression does not affect the MMS sensitivity of the other *tel1-Δ xxx-Δ* interactions suggests that there are additional telomere-length-independent defects that contribute to the MMS sensitivity of *tel1-Δ xxx-Δ* interactions.

tel1-Δ xxx-Δ interactions do not affect the frequency of NHEJ-mediated translocations

Lee *et al.* (2008) previously described an 11-fold increase in the frequency of DSB-induced, NHEJ-mediated translocations for a *tel1-Δ* mutant, reflecting a role for *TEL1* in preventing deleterious chromosomal fusions through an as-yet-undefined mechanism. That a *tel1-Δ* strain is not sensitive to DNA-damaging agents despite this defect suggests that the occurrence of these events even in the presence of DNA-damaging agents is a rarity. Thus, one possibility is that the *tel1-Δ xxx-Δ* interactions identified here may increase cellular dependence on *TEL1* to prevent deleterious chromosomal fusions. We tested this possibility by determining whether the *tel1-Δ xxx-Δ* double mutants experience enhanced frequencies (compared to *tel1*) of chromosomal translocations. We cloned each of the 13 single mutants and *tel1-Δ xxx-Δ* double mutants into a strain background harboring the translocation assay construct (Lee *et al.* 2008) that employs two *GAL*-inducible *HO* cuts on chromosomes V and VII, where each breakpoint contains a nonfunctional fragment of the *URA3* gene. Translocations are measured by the reconstitution of a functional *URA3* allele, which is dependent on Ku70/80-mediated NHEJ (Lee *et al.* 2008). We measured the frequency of translocations after the induction of *GAL-HO* for the panel of *tel1-Δ xxx-Δ* interaction strains (Figure 6). While we were able to reproduce the Ku-dependent increase in Ura^+ translocations for *tel1-Δ*, none of the other double mutants exhibited frequencies that differed from *tel1-Δ*. From this we conclude that an increased frequency of DSB-induced chromosomal translocations is unlikely to be the cause of the MMS sensitivity exhibited by *tel1-Δ xxx-Δ* interactions. This is supported by the fact that the *tel1-Δ xxx-Δ* MMS interactions were also largely insensitive to IR (Figure 1), which directly induces DSBs [whether or not MMS produces DSBs is a current source of controversy (Lundin *et al.* 2005)].

GCRs in tel1-Δ xxx-Δ strains

Kolodner and colleagues have previously shown that one double mutant identified in this screen (*rad24 tel1*) causes an increased frequency of spontaneous chromosome breakage and rearrangement involving the left arm of chromosome V (the GCR arrangement assay) (Myung and Kolodner 2002). As MMS has also been shown to induce higher GCR frequencies (Myung and Kolodner 2003; Stellwagen *et al.* 2003), we asked whether the MMS sensitivity exhibited by the *tel1-Δ xxx-Δ* double mutants may reflect an increased frequency of MMS-induced genome rearrangements. To do this, we grew single- and double-mutant strains in the presence of 0.003% MMS for 15 hr to induce GCR events, which were detected by selecting for the loss of two nearby markers (*CAN1* and *URA3*) on the left arm of chromosome V, as previously described (Chen and Kolodner 1999). The 0.003% MMS exposure resulted in an ~10-fold induction of GCR events for wild-type cells. For the *tel1-Δ xxx-Δ* double mutants, members of the 9-1-1 complex showed an ~300-fold induction of MMS-induced GCR events when combined with *tel1-Δ* (Figure 7A). The *rad27-Δ tel1-Δ* mutant and *nup60-Δ tel1-Δ* each showed a minor ~5-fold increase in MMS-induced GCR. None of

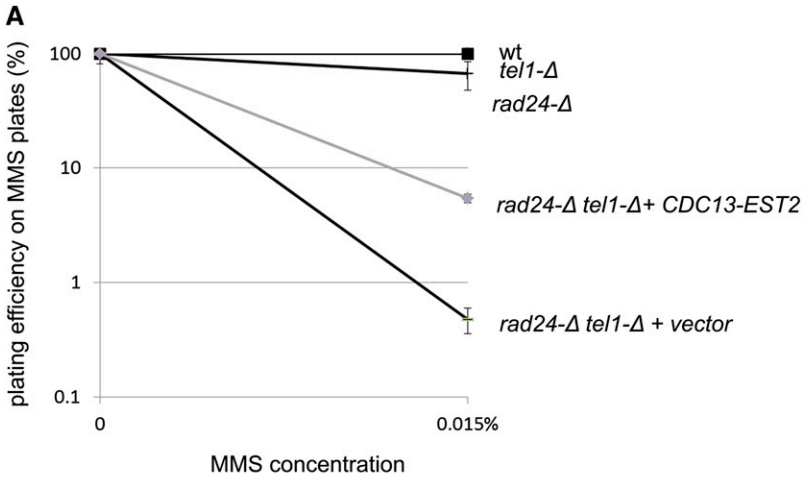

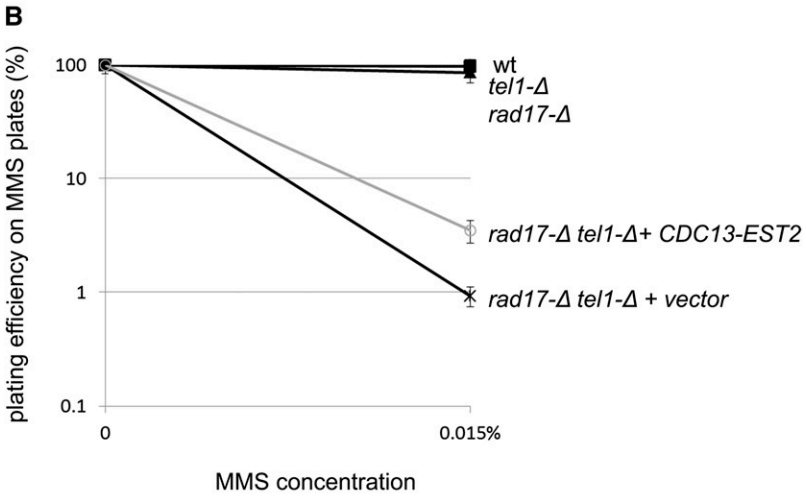

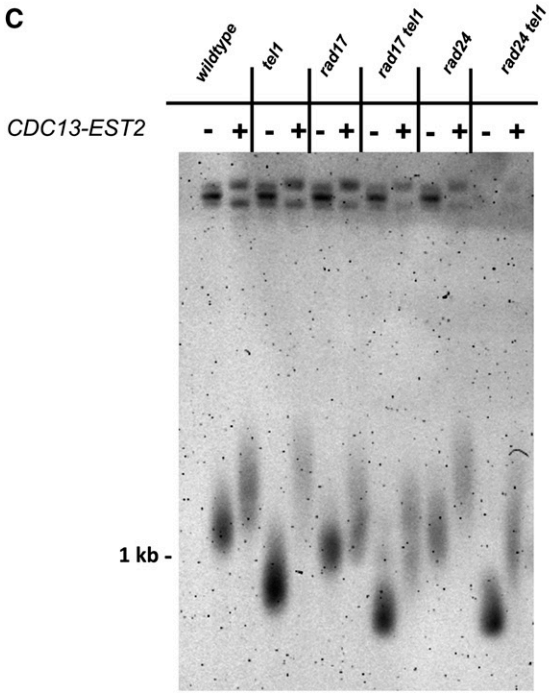

Figure 5 Suppression of MMS sensitivity in *rad24-Δ tel1-Δ* and *rad17-Δ tel1-Δ* by a *CDC13-EST2* fusion plasmid. (A and B) Strains of the indicated genotype were transformed either with an empty vector or with a *CDC13-EST*2 fusion plasmid (pVL1107) and screened for MMS sensitivity by colony-forming assay on MMS plates. Error bars represent the standard deviation of values from three independent transformants. (C) Telomere lengths for *tel1-*Δ interactions with or without the *CDC13-EST2* fusion plasmid. Cells with the *CDC13-EST2* fusion plasmid or empty vector were propagated on –Leu media and diluted in fresh rich medium overnight. Genomic DNA was harvested the following day and analyzed by electrophoresis and Southern blotting. The blot was probed with sequence complementary to a region in the Y′ subtelomeric element.

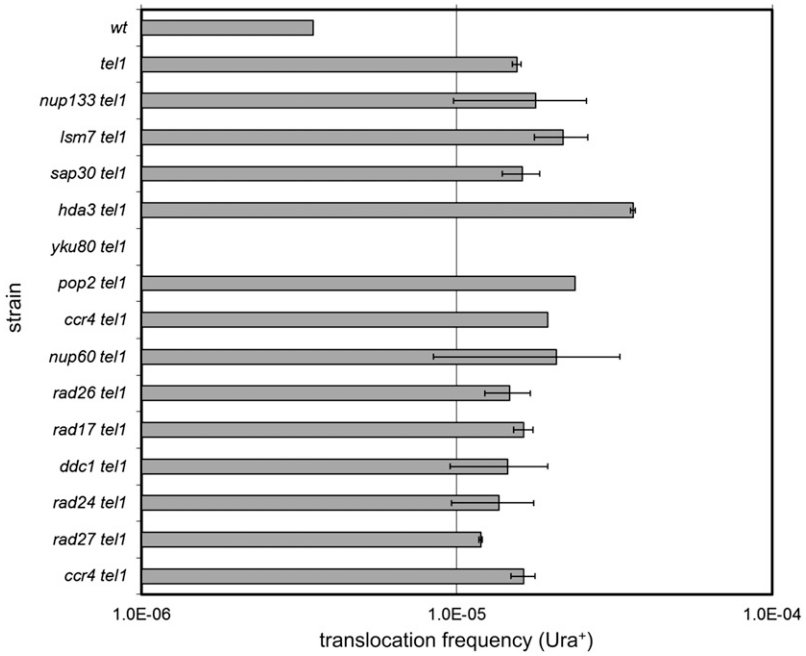

Figure 6 *HO*-induced translocation frequency for *tel1-Δ* interactions. NHEJ-mediated translocation frequency for *tel1*-Δ double mutants following *GAL-HO* induction of DSBs on chromosome V and chromosome VII. Frequencies are measured as the fraction of colonies that survive on −Ura plates. Error bars indicate the standard deviation of values from three independent transformants.

the other double mutants exhibited an increased GCR frequency (Figure 7A). From these data, we conclude that a subset of *tel1-Δ xxx-Δ* interactions (*rad17-Δ tel1-Δ*, *ddc1-Δ tel1-Δ*, *rad24-Δ tel1-Δ*, *rad27-Δ tel1-Δ*, and *nup60-Δ tel1-Δ*) exhibit increased genome instability as measured by the GCR assay.

As restoration of telomere lengths through addition of the *CDC13-EST2* fusion plasmid restored a proportion of MMS resistance to the *9-1-1-Δ tel1-Δ* mutant strains, we asked whether the *CDC13-EST2* fusion would also suppress the increased MMS-induced GCR frequency of a *9-1-1-Δ tel1-Δ* mutant as well. We tested a *rad17-Δ tel1-Δ* mutant along with the corresponding single mutants for the induction of GCR events with or without the fusion construct. As can be seen in Figure 7B, the *rad17-Δ tel1-Δ* double-mutant strain harboring the fusion plasmid had a reduced GCR frequency relative to the same strain carrying an empty vector. Consistent with a partial reduction in MMS sensitivity, the *CDC13-EST2* fusion did not completely abolish MMS-induced gross chromosomal rearrangements in the *rad17-Δ tel1-Δ* strain. From these data, we conclude that a proportion of the MMS sensitivity exhibited by *9-1-1-Δ tel1-Δ* strains is due to MMS-induced genomic instability that is caused by telomere shortening. However, much of the increased GCR in *9-1-1-Δ tel1-Δ* is unexplained by telomere length effects; thus additional mechanisms (*i.e.*, aside from altered telomere length) contribute to the sensitivity of *tel1-Δ xxx-Δ* interactions.

A tel1-Δ strain is rendered sensitive to MMS by predepletion of nucleotide pools

Prior studies have implicated both the *9-1-1* complex and the CCR4-NOT complex as key regulators of ribonucleotide reductase, and mutants in these pathways exhibit depleted nucleotide pools and are sensitive to replication stress (Zhao *et al.* 2001; Westmoreland *et al.* 2004; Mulder *et al.* 2005; Traven *et al.* 2005; Woolstencroft *et al.* 2006). Moreover, a *ccr4-Δ tel1-Δ* strain has been previously shown to exhibit enhanced sensitivity to the ribonucleotide reductase inhibitor hydroxyurea (Woolstencroft *et al.* 2006). Thus we hypothesized that a decrease in dNTP pools in *9-1-1-Δ tel1-Δ* and *ccr4-Δ/pop2-Δ tel1-Δ* may contribute to the MMS sensitivity exhibited by these strains. From this, we predicted that depletion of nucleotide pools (*e.g.*, by pretreating cells with hydroxyurea) in *tel1-Δ* cells should phenocopy deletion of *CCR4* in a *tel1-Δ* background, thus sensitizing *tel1-Δ* cells to MMS. To test this prediction, wild-type and *tel1-Δ* cells were cultured in rich medium with 0, 50, or 150 mM HU for a period of 4 hr, after which the HU was removed, and cells were plated onto MMS plates to assess viability. As expected, the MMS sensitivity of a wild-type strain does not change, regardless of whether the cells have been pretreated with HU (Figure 8). In contrast, while a *tel1-Δ* strain is insensitive to the HU pretreatment alone, when HU pretreatment is followed by plating on MMS plates, *tel1-Δ* cells exhibit enhanced MMS sensitivity in a dose-dependent manner, with the greatest MMS sensitivity observed in 150 mM HU (Figure 8). From this we conclude that depletion of nucleotide pools renders *tel1-Δ* sensitive to the DNA-damaging agent MMS, consistent with a model in which increased replication stress contributes to the MMS sensitivity exhibited by the *9-1-1-Δ tel1-Δ* and ccr4-Δ *tel1-Δ/pop2-Δ tel1-Δ* mutants (and possibly other *tel1-Δ xxx-Δ* double mutants isolated in the screen; see *Discussion*).

Discussion

Categorizing the tel1-Δ interactions

While a *tel1-Δ* mutant exhibits interactions with a diverse set of 13 mutants, we found that these interactions fell into

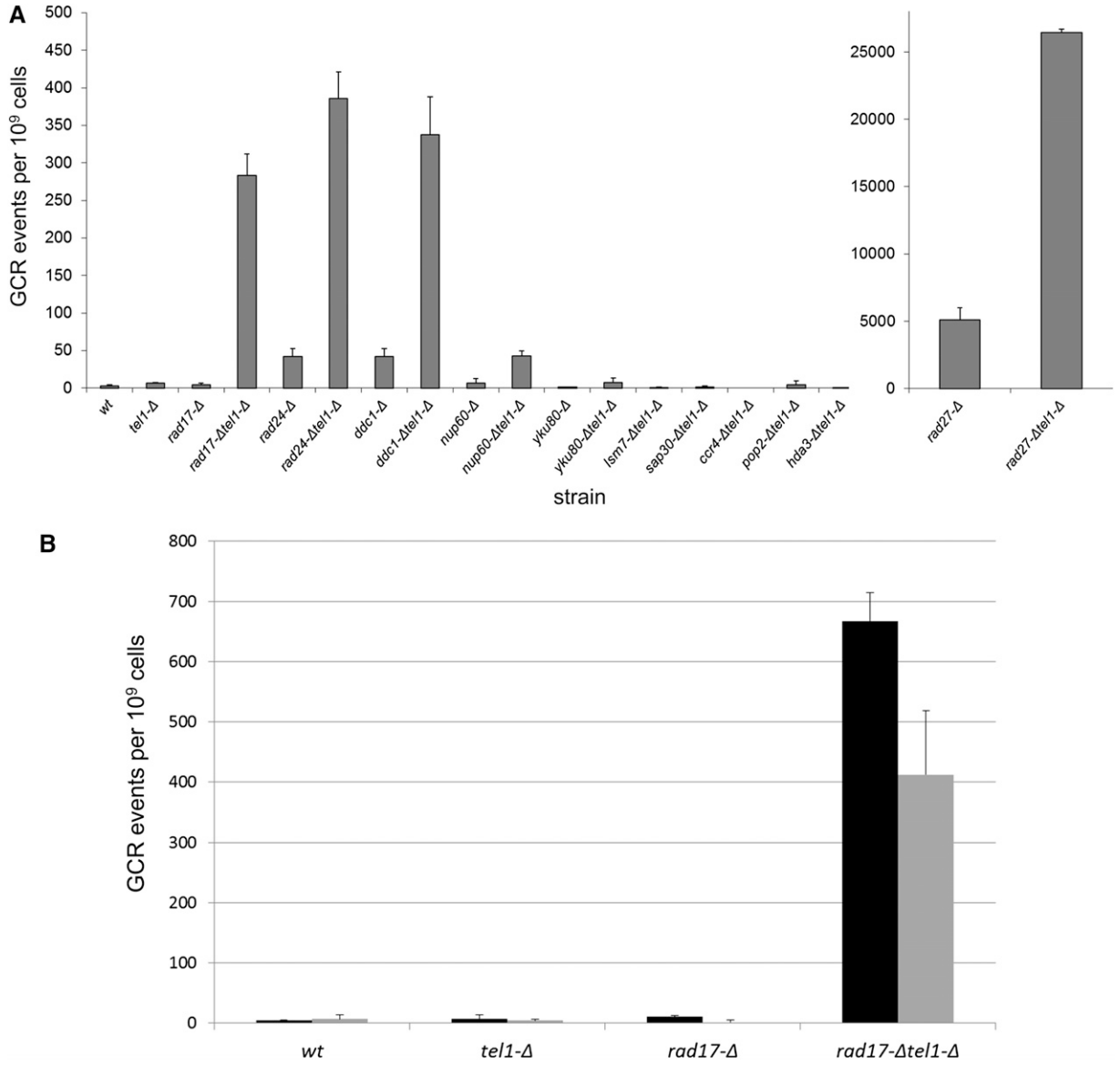

Figure 7 GCR frequency in 0.003% MMS. (A) GCR frequency for *tel1-Δ* interactions. Strains were grown in YEPD + 0.003% MMS for 15 hr and subsequently plated onto C-Arg-Ser + canavanine + 5-FOA to simultaneously select for the loss of *CAN1* and *URA3* markers on the left end of chromosome V. Error bars represent standard deviations from two independent cultures per strain, each plated two times. The *rad27-Δ* mutants are plotted separately due to scale. (B) GCR frequency in 0.003% MMS with or without the *CDC13-EST2* fusion plasmid. The indicated strains containing either an empty vector (black bars) or the *CDC13-EST2* fusion (gray bars) were grown in YEPD + 0.003% MMS for 15 hr and subsequently plated onto C-Arg-Ser + canavanine + 5-FOA to select for simultaneous loss of *CAN1* and *URA3* markers. Error bars represent standard deviations from two independent cultures per strain, each plated two times.

three phenotypic classes based upon our follow-up characterizations (Table 2). The first class is composed of mutants in the 9-1-1 complex (*rad17-Δ* and *ddc1-Δ*) and the 9-1-1 clamp loader (*rad24-Δ*); these *tel1-Δ* interactions conferred a rather large (>100-fold) increase in MMS sensitivity (Figure 1A), cross-sensitivity to IR (Figure 1, B and C), a pronounced telomere defect (Figure 3), and a synergistic increase in GCR events (Figure 7). For this class, the DNA damage sensitivity and the increase in GCR frequencies were partially suppressed by elongating telomeres using the *CDC13-EST2* fusion construct (Figures 5 and 7B). The second class of interactions comprises *ccr4-Δ*, *pop2-Δ*, *sap30-Δ*, *hda3-Δ*, *yku80-Δ*, *rad27-Δ*, *nup133-Δ*, and *nup60-Δ* (Table 2); these exhibited a somewhat milder interaction with *tel1-Δ* in MMS and no cross-sensitive interactions to IR, but exhibited a discernible telomere length defect with *tel1-Δ* (Figure 3). The third class of mutants, *rad26-Δ* and *lsm7-Δ*, showed similar characteristics to class 2, but did not exhibit any discernible telomere length defect (Figure 3). There is likely some overlap between these classes in the mechanism that causes their interactions with *tel1-Δ* (discussed below).

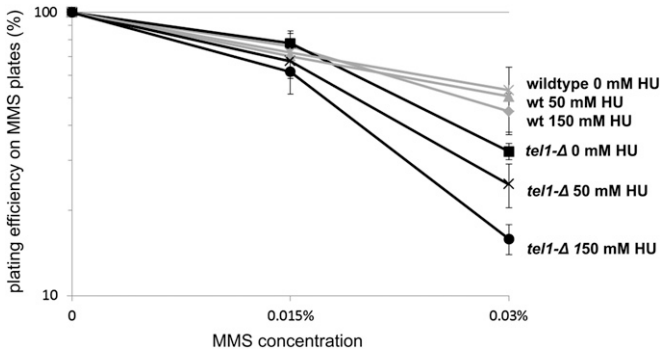

Figure 8 MMS sensitivity following pretreatment with HU. The indicated strains were grown in the presence of the indicated dose of HU for 4 hr to deplete nucleotide pools. Cells were then washed two times and plated onto MMS plates to assay MMS sensitivity by colony-forming assay. The error bars indicate the standard deviation of values from three independent cultures.

A replication defect underlies sensitivity to MMS in multiple classes of tel1-Δ interactions

While the *tel1-Δ* interactions composing classes 1 and 2 (Table 2) exhibit shortened telomeres relative to the corresponding single mutants, only in the class 1 case is MMS sensitivity suppressed by telomere elongation (Figure 5), and even in this class of double mutants the suppression is modest. While it is formally possible that telomere elongation due to the expression of the *CDC13-EST2* fusion creates a structure that is somehow physiologically different from a natural telomere and thus is not a good substitute, a more straightforward model is that only a minor proportion of MMS sensitivity is directly caused by telomere shortening in class 1 mutants, while the majority of MMS sensitivity in these and other *tel1-Δ xxx-Δ* interactions reflects an underlying replication defect that manifests a dual-pronged effect on telomere metabolism and MMS resistance.

Our data (and other studies) support a model in which increased replication stress, combined with a *tel1-Δ*-mediated defect in replication fork stability, causes both MMS sensitivity and telomere shortening in *tel1-Δ xxx-Δ* interactions. First, aside from a modest effect in the class 1 mutants, none of the identified in *tel1-Δ xxx-Δ* interactions exhibit cross-sensitivity to ionizing radiation, regardless of whether the IR was administered as a pulse (Figure 1B) or as chronic treatment (Figure 1C). Unlike MMS treatment, IR does not induce detectable replication fork stalling (Merrick *et al.* 2004), so while there is a minor IR interaction in *tel1-Δ 9-1-1-Δ* cells (Figure 1, B and C) (likely through an additive defect in Mec1/Tel1 DSB sensing), replication fork stalling/collapse is the likely major lethal lesion in *tel1-Δ xxx-Δ* interactions. Additionally, recent studies have uncovered a *TEL1*-dependent role in the preservation of fork stability through the prevention of fork reversion and degradation into abnormal cruciform structures (Doksani *et al.* 2009). Consistent with this, Kaochar *et al.* (2010) showed that *tel1-Δ* exhibits an increased frequency of dicentric chromosomes due to the fusion of inverted repeats likely due to fork reversion. As the reason why *tel1-Δ* cells exhibit short telomeres is poorly understood, it is formally possible that a failure to preserve fork stability in telomeric regions in *tel1-Δ* cells is causative for the short telomere phenotype [telomeres are enriched for replication pause sites such as G-quadruplex structures (Ivessa *et al.* 2002; Bochman *et al.* 2012)].

Many of the *tel1-Δ* interactions identified in the MMS screen fit a model for increased replication stress. Members of class 1 (9-1-1 components) (Table 2) are required for the *MEC1*-dependent degradation of the ribonucleotide reductase inhibitor Sml1 following MMS treatment (Zhao *et al.* 2001; Chabes *et al.* 2003); the resultant increase in dNTP production following this process is thought to facilitate DNA synthesis at stalled forks to prevent fork collapse (Fasullo *et al.* 2010). In addition, members of class 2 (*CCR4* and *POP2*, members of the CCR4-NOT deadenylation complex) are known regulators of ribonucleotide reductase, and mutants in *ccr4-Δ* and *pop2-Δ* are sensitive to replication inhibitors such as HU (Westmoreland *et al.* 2004; Mulder *et al.* 2005; Traven *et al.* 2005; Woolstencroft

Table 2 Tabulation of phenotypes for *tel1-Δ* interactions identified in the MMS screen

	Strain	MMS interaction	IR interaction	GCR	Short telomere	*CDC13-EST2* rescue	Description
Class 1	*rad24-Δtel1-Δ*	++	+	++	++	+/−	9-1-1 complex
	rad17-Δtel1-Δ	++	+	++	++	+/−	9-1-1 complex
	ddc1-Δtel1-Δ	++	+	++	++	+/−	9-1-1 complex
Class 2	*nup60-Δtel1-Δ*	+	—	+	+	—	Nucleoporin
	rad27-Δtel1-Δ	+	—	+	+	—	Flap endonuclease
	sap30-Δtel1-Δ	+	—	—	+	—	Deacetylase
	pop2-Δtel1-Δ	+	—	—	+	—	Deadenylase
	ccr4-Δtel1-Δ	+	—	—	+	—	Deadenylase
	hda3-Δtel1-Δ	+	—	—	+	—	deacetylase
	yku80-Δtel1-Δ	+	—	—	+	—	NHEJ
	nup133-Δtel1-Δ	+	—	—	+	—	Nucleoporin
Class 3	*lsm7-Δtel1-Δ*	+	—	—	—	—	mRNA decap
	rad26-Δtel1-Δ	+	—	—	—	—	TCR

For each of the *tel1-Δ xxx-Δ* genetic interactions identified in the MMS screen a "+" indicates whether a double mutant exhibited a positive result in each of the assays tested (*e.g.*, increased GCR frequency, shorter telomere, etc.); a "++" indicates a more severe phenotype; and a "+/−" indicates partial suppression. TCR, transcription-coupled repair.

et al. 2006). As telomere shortening has recently been shown to occur upon dNTP depletion (Gupta *et al.* 2013), it is likely that the short telomeres in CCR4-NOT and 9-1-1 mutants are at least partially due to this mechanism. Consistent with a model for increased replication stress in *tel1-Δ xxx-Δ* cells, depleting nucleotide pools by pretreatment with HU (effectively phenocopying the loss of *9-1-1* or *CCR4/POP2*) sensitizes *tel1-Δ* cells to MMS in a dose-dependent manner, whereas a wild-type strain is unaffected by the HU pretreatment (Figure 8).

Other mutants composing class 2 are also linked to preventing replication stress via counteracting fork regression [*RAD27* (Kang *et al.* 2010)] or stabilizing sites of active transcription [*NUP60/NUP133* (Palancade *et al.* 2007; Bermejo *et al.* 2011)]. Additionally, the mutants composing class 3 (Table 2) are linked to increased replication stress due to defects in histone regulation [*LSM7* (Herrero and Moreno 2011; Tkach *et al.* 2012)] or through defective targeting of transcription-coupled repair [*RAD26* (Kapitzky *et al.* 2010; Malik *et al.* 2010)].

Progressive telomere shortening is a cause for MMS sensitivity

Recently, numerous studies have described a connection between short telomeres and enhanced sensitivity to DNA-damaging agents across a variety of organisms (Wong *et al.* 2000; Lin *et al.* 2009; Soler *et al.* 2009; Drissi *et al.* 2011); the reason for this relationship is poorly understood. Here, we show that, in yeast, cellular sensitivity to MMS progressively increases as telomeres shorten (Figure 2), suggesting that the progressive loss of telomere protection renders cells sensitive to MMS. In concordance with this, a proportion of MMS sensitivity and genome instability can be suppressed in *9-1-1-Δ tel1-Δ* mutants by alleviating the short telomere phenotype in these cells (Figures 5 and 7B).

There are multiple possible mechanisms for how short telomeres cause MMS sensitivity. Loss of telomeric protection can render telomeres as targets for the DDR, and the loss of telomerase activity is associated with a gradual increase in constitutive Rad53 phosphorylation (Grandin *et al.* 2005); accordingly, in telomerase-deficient cells telomeres are enriched for DDR proteins while nontelomeric DSBs exhibit reduced binding of DDR factors (Lin *et al.* 2009). Thus, the recruitment of DDR factors to short telomeres may interfere with the ability of the cell to cope with MMS-induced stress elsewhere in the genome. Alternatively, de-protected telomeres themselves may be problematic in the presence of MMS due to the potential for lethal chromosomal fusions with DSBs resulting from MMS-induced collapsed forks. Supporting this, a subset of GCR events can be suppressed by elongating telomeres in *9-1-1-Δ tel1-Δ* (Figure 7B), and a previous study has shown that a *9-1-1-Δ tel1-Δ* double mutant exhibits an increased frequency of spontaneous telomere–telomere fusions that can also be suppressed by elongating telomeres (Mieczkowski *et al.* 2003).

For the other identified interactions (class 2, Table 2), despite a lack of MMS suppression by *CDC13-EST2*, the telomere defect in these cells may still be a cause of MMS sensitivity. For example, an increase in ssDNA at telomeres would create a structure that is more susceptible to MMS-induced lesions [fork-blocking lesions occur predominantly in ssDNA in MMS (Shrivastav *et al.* 2010)]. Accordingly, a *rad27* mutant is associated with abnormally large regions of ssDNA in telomeres (Parenteau and Wellinger 1999). As DNA damage in telomeres has recently been shown to be uniquely irreparable (Fumagalli *et al.* 2012), it is likely that telomeres exhibiting abnormal structures are both more susceptible to MMS-induced damage and less able to survive it.

Implications of the tel1-Δ screen for mammalian cells

From this study, we show that *tel1-Δ* cells are rendered sensitive to MMS by increased replication stress or exacerbation of the short telomere phenotype. Thus, targeting these mechanisms may be an effective strategy for killing tumor cells that have lost ATM activity. Intriguingly, a recent study found that the specific combination of an *ATM* (*TEL1* ortholog) inhibitor drug combined with a telomerase inhibitor rendered tumor cells extremely sensitive to the chemotherapy agent etoposide (Tamakawa *et al.* 2010). Furthermore, based on the replication stress model described above, targeting ATM for inhibition, combined with agents such as MMS, would be expected to confer a synergistic effect in cells experiencing oncogene-induced replication stress.

Acknowledgments

We thank Brenda Andrews, Charles Boone, Daniel Gottschling, Vicki Lundblad, and Sang Eun Lee for strains and plasmids used in this study and Mary Ellard-Ivey for access to equipment. We thank members of the Brewer/Raghuraman and Gottschling labs and Wenyi Feng and Lindsey Williams for helpful discussions related to this study. We thank our anonymous reviewers and the *GENETICS* Editor for helpful comments on the manuscript. B.D.P. was supported by the Fred Hutchinson Cancer Research Center Dual Mentor Program and a U.S. Department of Defense Breast Cancer Research Program predoctoral fellowship. This work was supported by National Institutes of Health grant R01 CA 129604.

Literature Cited

Agarwal, M., S. Pandita, C. R. Hunt, A. Gupta, X. Yue *et al.*, 2008 Inhibition of telomerase activity enhances hyperthermia-mediated radiosensitization. Cancer Res. 68: 3370–3378.

Arneric, M., and J. Lingner, 2007 Tel1 kinase and subtelomere-bound Tbf1 mediate preferential elongation of short telomeres by telomerase in yeast. EMBO Rep. 8: 1080–1085.

Bermejo, R., T. Capra, R. Jossen, A. Colosio, C. Frattini *et al.*, 2011 The replication checkpoint protects fork stability by releasing transcribed genes from nuclear pores. Cell 146: 233–246.

Bochman, M. L., K. Paeschke, and V. A. Zakian, 2012 DNA secondary structures: stability and function of G-quadruplex structures. Nat. Rev. Genet. 13: 770–780.

Brachmann, C. B., A. Davies, G. J. Cost, E. Caputo, J. Li *et al.*, 1998 Designer deletion strains derived from *Saccharomyces cerevisiae* S288C: a useful set of strains and plasmids for PCR-mediated gene disruption and other applications. Yeast 14: 115–132.

Canman, C. E., D. S. Lim, K. A. Cimprich, Y. Taya, K. Tamai *et al.*, 1998 Activation of the ATM kinase by ionizing radiation and phosphorylation of p53. Science 281: 1677–1679.

Chabes, A., B. Georgieva, V. Domkin, X. Zhao, R. Rothstein *et al.*, 2003 Survival of DNA damage in yeast directly depends on increased dNTP levels allowed by relaxed feedback inhibition of ribonucleotide reductase. Cell 112: 391–401.

Chang, M., M. Arneric, and J. Lingner, 2007 Telomerase repeat addition processivity is increased at critically short telomeres in a Tel1-dependent manner in *Saccharomyces cerevisiae*. Genes Dev. 21: 2485–2494.

Chapon, C., T. R. Cech, and A. J. Zaug, 1997 Polyadenylation of telomerase RNA in budding yeast. RNA 3: 1337–1351.

Chen, C., and R. D. Kolodner, 1999 Gross chromosomal rearrangements in *Saccharomyces cerevisiae* replication and recombination defective mutants. Nat. Genet. 23: 81–85.

Cimprich, K. A., T. B. Shin, C. T. Keith, and S. L. Schreiber, 1996 cDNA cloning and gene mapping of a candidate human cell cycle checkpoint protein. Proc. Natl. Acad. Sci. USA 93: 2850–2855.

Craven, R. J., P. W. Greenwell, M. Dominska, and T. D. Petes, 2002 Regulation of genome stability by *TEL1* and *MEC1*, yeast homologs of the mammalian *ATM* and *ATR* genes. Genetics 161: 493–507.

Doksani, Y., R. Bermejo, S. Fiorani, J. E. Haber, and M. Foiani, 2009 Replicon dynamics, dormant origin firing, and terminal fork integrity after double-strand break formation. Cell 137: 247–258.

Drissi, R., J. Wu, Y. Hu, C. Bockhold, and J. S. Dome, 2011 Telomere shortening alters the kinetics of the DNA damage response after ionizing radiation in human cells. Cancer Prev. Res. (Phila.) 4: 1973–1981.

Evans, S. K., and V. Lundblad, 1999 Est1 and Cdc13 as comediators of telomerase access. Science 286: 117–120.

Fasullo, M., O. Tsaponina, M. Sun, and A. Chabes, 2010 Elevated dNTP levels suppress hyper-recombination in *Saccharomyces cerevisiae* S-phase checkpoint mutants. Nucleic Acids Res. 38: 1195–1203.

Fukunaga, K., Y. Kwon, P. Sung, and K. Sugimoto, 2011 Activation of protein kinase Tel1 through recognition of protein-bound DNA ends. Mol. Cell. Biol. **31:** 1959–1971.

Fumagalli, M., F. Rossiello, M. Clerici, S. Barozzi, D. Cittaro *et al.*, 2012 Telomeric DNA damage is irreparable and causes persistent DNA-damage-response activation. Nat. Cell Biol. 14: 355–365.

Gao, H., T. B. Toro, M. Paschini, B. Braunstein-Ballew, R. B. Cervantes *et al.*, 2010 Telomerase recruitment in *Saccharomyces cerevisiae* is not dependent on Tel1-mediated phosphorylation of Cdc13. Genetics 186: 1147–1159.

Gonzalez-Suarez, E., F. A. Goytisolo, J. M. Flores, and M. A. Blasco, 2003 Telomere dysfunction results in enhanced organismal sensitivity to the alkylating agent N-methyl-N-nitrosourea. Cancer Res. 63: 7047–7050.

Goytisolo, F. A., E. Samper, J. Martin-Caballero, P. Finnon, E. Herrera *et al.*, 2000 Short telomeres result in organismal hypersensitivity to ionizing radiation in mammals. J. Exp. Med. 192: 1625–1636.

Grandin, N., A. Bailly, and M. Charbonneau, 2005 Activation of Mrc1, a mediator of the replication checkpoint, by telomere erosion. Biol. Cell 97: 799–814.

Greenwell, P. W., S. L. Kronmal, S. E. Porter, J. Gassenhuber, B. Obermaier *et al.*, 1995 *TEL1*, a gene involved in controlling telomere length in *S. cerevisiae*, is homologous to the human ataxia telangiectasia gene. Cell 82: 823–829.

Gupta, A., S. Sharma, P. Reichenbach, L. Marjavaara, A. K. Nilsson *et al.*, 2013 Telomere length homeostasis responds to changes in intracellular dNTP pools. Genetics 193: 1095–1105.

Herrero, A. B., and S. Moreno, 2011 Lsm1 promotes genomic stability by controlling histone mRNA decay. EMBO J. 30: 2008–2018.

Ivessa, A. S., J. Q. Zhou, V. P. Schulz, E. K. Monson, and V. A. Zakian, 2002 *Saccharomyces* Rrm3p, a 5′ to 3′ DNA helicase that promotes replication fork progression through telomeric and subtelomeric DNA. Genes Dev. 16: 1383–1396.

Kang, M. J., C. H. Lee, Y. H. Kang, I. T. Cho, T. A. Nguyen *et al.*, 2010 Genetic and functional interactions between Mus81-Mms4 and Rad27. Nucleic Acids Res. 38: 7611–7625.

Kaochar, S., L. Shanks, and T. Weinert, 2010 Checkpoint genes and Exo1 regulate nearby inverted repeat fusions that form dicentric chromosomes in *Saccharomyces cerevisiae*. Proc. Natl. Acad. Sci. USA 107: 21605–21610.

Kapitzky, L., P. Beltrao, T. J. Berens, N. Gassner, C. Zhou *et al.*, 2010 Cross-species chemogenomic profiling reveals evolutionarily conserved drug mode of action. Mol. Syst. Biol. 6: 451.

Kastan, M. B., Q. Zhan, W. S. el-Deiry, F. Carrier, T. Jacks *et al.*, 1992 A mammalian cell cycle checkpoint pathway utilizing p53 and GADD45 is defective in ataxia-telangiectasia. Cell 71: 587–597.

Kuhne, M., E. Riballo, N. Rief, K. Rothkamm, P. A. Jeggo *et al.*, 2004 A double-strand break repair defect in *ATM*-deficient cells contributes to radiosensitivity. Cancer Res. 64: 500–508.

Lee, J. H., and T. T. Paull, 2007 Activation and regulation of ATM kinase activity in response to DNA double-strand breaks. Oncogene 26: 7741–7748.

Lee, K., Y. Zhang, and S. E. Lee, 2008 *Saccharomyces cerevisiae* ATM orthologue suppresses break-induced chromosome translocations. Nature 454: 543–546.

Lin, Y. H., C. C. Chang, C. W. Wong, and S. C. Teng, 2009 Recruitment of Rad51 and Rad52 to short telomeres triggers a Mec1-mediated hypersensitivity to double-stranded DNA breaks in senescent budding yeast. PLoS ONE 4: e8224.

Longhese, M. P., V. Paciotti, H. Neecke, and G. Lucchini, 2000 Checkpoint proteins influence telomeric silencing and length maintenance in budding yeast. Genetics 155: 1577–1591.

Lundin, C., M. North, K. Erixon, K. Walters, D. Jenssen *et al.*, 2005 Methyl methanesulfonate (MMS) produces heat-labile DNA damage but no detectable in vivo DNA double-strand breaks. Nucleic Acids Res. 33: 3799–3811.

Lustig, A. J., and T. D. Petes, 1986 Identification of yeast mutants with altered telomere structure. Proc. Natl. Acad. Sci. USA 83: 1398–1402.

Malik, S., P. Chaurasia, S. Lahudkar, G. Durairaj, A. Shukla *et al.*, 2010 Rad26p, a transcription-coupled repair factor, is recruited to the site of DNA lesion in an elongating RNA polymerase II-dependent manner in vivo. Nucleic Acids Res. 38: 1461–1477.

Mallory, J. C., and T. D. Petes, 2000 Protein kinase activity of Tel1p and Mec1p, two *Saccharomyces cerevisiae* proteins related to the human ATM protein kinase. Proc. Natl. Acad. Sci. USA 97: 13749–13754.

Mantiero, D., M. Clerici, G. Lucchini, and M. P. Longhese, 2007 Dual role for *Saccharomyces cerevisiae* Tel1 in the checkpoint response to double-strand breaks. EMBO Rep. 8: 380–387.

Marcand, S., E. Gilson, and D. Shore, 1997 A protein-counting mechanism for telomere length regulation in yeast. Science 275: 986–990.

Martina, M., M. Clerici, V. Baldo, D. Bonetti, G. Lucchini *et al.*, 2012 A balance between Tel1 and Rif2 activities regulates nucleolytic processing and elongation at telomeres. Mol. Cell. Biol. 32: 1604–1617.

McCulley, J. L., and T. D. Petes, 2010 Chromosome rearrangements and aneuploidy in yeast strains lacking both Tel1p and Mec1p reflect deficiencies in two different mechanisms. Proc. Natl. Acad. Sci. USA 107: 11465–11470.

McGee, J. S., J. A. Phillips, A. Chan, M. Sabourin, K. Paeschke *et al.*, 2010 Reduced Rif2 and lack of Mec1 target short telomeres for elongation rather than double-strand break repair. Nat. Struct. Mol. Biol. 17: 1438–1445.

Merrick, C. J., D. Jackson, and J. F. Diffley, 2004 Visualization of altered replication dynamics after DNA damage in human cells. J. Biol. Chem. 279: 20067–20075.

Metcalfe, J. A., J. Parkhill, L. Campbell, M. Stacey, P. Biggs *et al.*, 1996 Accelerated telomere shortening in ataxia telangiectasia. Nat. Genet. 13: 350–353.

Mieczkowski, P. A., J. O. Mieczkowska, M. Dominska, and T. D. Petes, 2003 Genetic regulation of telomere-telomere fusions in the yeast *Saccharomyces cerevisae*. Proc. Natl. Acad. Sci. USA 100: 10854–10859.

Morrow, D. M., D. A. Tagle, Y. Shiloh, F. S. Collins, and P. Hieter, 1995 *TEL1*, an *S. cerevisiae* homolog of the human gene mutated in ataxia telangiectasia, is functionally related to the yeast checkpoint gene *MEC1*. Cell 82: 831–840.

Mulder, K. W., G. S. Winkler, and H. T. Timmers, 2005 DNA damage and replication stress induced transcription of *RNR* genes is dependent on the Ccr4-Not complex. Nucleic Acids Res. 33: 6384–6392.

Murakami-Sekimata, A., D. Huang, B. D. Piening, C. Bangur, and A. G. Paulovich, 2010 The *Saccharomyces cerevisiae RAD9*, *RAD17* and *RAD24* genes are required for suppression of mutagenic post-replicative repair during chronic DNA damage. DNA Repair (Amst.) 9: 824–834.

Myung, K., and R. D. Kolodner, 2002 Suppression of genome instability by redundant S-phase checkpoint pathways in *Saccharomyces cerevisiae*. Proc. Natl. Acad. Sci. USA 99: 4500–4507.

Myung, K., and R. D. Kolodner, 2003 Induction of genome instability by DNA damage in *Saccharomyces cerevisiae*. DNA Repair (Amst.) 2: 243–258.

Nakada, D., K. Matsumoto, and K. Sugimoto, 2003 *ATM*-related Tel1 associates with double-strand breaks through an Xrs2-dependent mechanism. Genes Dev. 17: 1957–1962.

Nakamura, M., K. Masutomi, S. Kyo, M. Hashimoto, Y. Maida *et al.*, 2005 Efficient inhibition of human telomerase reverse transcriptase expression by RNA interference sensitizes cancer cells to ionizing radiation and chemotherapy. Hum. Gene Ther. 16: 859–868.

Paciotti, V., M. Clerici, G. Lucchini, and M. P. Longhese, 2000 The checkpoint protein Ddc2, functionally related to *S. pombe* Rad26, interacts with Mec1 and is regulated by Mec1-dependent phosphorylation in budding yeast. Genes Dev. 14: 2046–2059.

Painter, R. B., and B. R. Young, 1980 Radiosensitivity in ataxia-telangiectasia: a new explanation. Proc. Natl. Acad. Sci. USA 77: 7315–7317.

Palancade, B., X. Liu, M. Garcia-Rubio, A. Aguilera, X. Zhao *et al.*, 2007 Nucleoporins prevent DNA damage accumulation by modulating Ulp1-dependent sumoylation processes. Mol. Biol. Cell 18: 2912–2923.

Parenteau, J., and R. J. Wellinger, 1999 Accumulation of single-stranded DNA and destabilization of telomeric repeats in yeast mutant strains carrying a deletion of *RAD27*. Mol. Cell. Biol. 19: 4143–4152.

Paulovich, A. G., C. D. Armour, and L. H. Hartwell, 1998 The *Saccharomyces cerevisiae RAD9*, *RAD17*, *RAD24* and *MEC3* genes are required for tolerating irreparable, ultraviolet-induced DNA damage. Genetics 150: 75–93.

Ritchie, K. B., J. C. Mallory, and T. D. Petes, 1999 Interactions of *TLC1* (which encodes the RNA subunit of telomerase), *TEL1*, and *MEC1* in regulating telomere length in the yeast *Saccharomyces cerevisiae*. Mol. Cell. Biol. 19: 6065–6075.

Sabourin, M., C. T. Tuzon, and V. A. Zakian, 2007 Telomerase and Tel1p preferentially associate with short telomeres in *S. cerevisiae*. Mol. Cell 27: 550–561.

Savitsky, K., S. Sfez, D. A. Tagle, Y. Ziv, A. Sartiel *et al.*, 1995 The complete sequence of the coding region of the *ATM* gene reveals similarity to cell cycle regulators in different species. Hum. Mol. Genet. 4: 2025–2032.

Shiloh, Y., 2003 ATM and related protein kinases: safeguarding genome integrity. Nat. Rev. Cancer 3: 155–168.

Shrivastav, N., D. Li, and J. M. Essigmann, 2010 Chemical biology of mutagenesis and DNA repair: cellular responses to DNA alkylation. Carcinogenesis 31: 59–70.

Singer, M. S., and D. E. Gottschling, 1994 *TLC1*: template RNA component of *Saccharomyces cerevisiae* telomerase. Science 266: 404–409.

Singer, M. S., A. Kahana, A. J. Wolf, L. L. Meisinger, S. E. Peterson *et al.*, 1998 Identification of high-copy disruptors of telomeric silencing in *Saccharomyces cerevisiae*. Genetics 150: 613–632.

Soler, D., J. Pampalona, L. Tusell, and A. Genesca, 2009 Radiation sensitivity increases with proliferation-associated telomere dysfunction in nontransformed human epithelial cells. Aging Cell 8: 414–425.

Stellwagen, A. E., Z. W. Haimberger, J. R. Veatch, and D. E. Gottschling, 2003 Ku interacts with telomerase RNA to promote telomere addition at native and broken chromosome ends. Genes Dev. 17: 2384–2395.

Tamakawa, R. A., H. B. Fleisig, and J. M. Wong, 2010 Telomerase inhibition potentiates the effects of genotoxic agents in breast and colorectal cancer cells in a cell cycle-specific manner. Cancer Res. 70: 8684–8694.

Teixeira, M. T., M. Arneric, P. Sperisen, and J. Lingner, 2004 Telomere length homeostasis is achieved via a switch between telomerase-extendible and -nonextendible states. Cell 117: 323–335.

Tkach, J. M., A. Yimit, A. Y. Lee, M. Riffle, M. Costanzo *et al.*, 2012 Dissecting DNA damage response pathways by analysing protein localization and abundance changes during DNA replication stress. Nat. Cell Biol. 14: 966–976.

Tong, A. H., and C. Boone, 2006 Synthetic genetic array analysis in *Saccharomyces cerevisiae*. Methods Mol. Biol. 313: 171–192.

Tong, A. H., M. Evangelista, A. B. Parsons, H. Xu, G. D. Bader *et al.*, 2001 Systematic genetic analysis with ordered arrays of yeast deletion mutants. Science (New York, N.Y.) 294: 2364–2368.

Traven, A., A. Hammet, N. Tenis, C. L. Denis, and J. Heierhorst, 2005 Ccr4-not complex mRNA deadenylase activity contributes to DNA damage responses in *Saccharomyces cerevisiae*. Genetics 169: 65–75.

Tsukamoto, Y., A. K. Taggart, and V. A. Zakian, 2001 The role of the Mre11-Rad50-Xrs2 complex in telomerase-mediated lengthening of *Saccharomyces cerevisiae* telomeres. Curr. Biol. 11: 1328–1335.

Vernon, M., K. Lobachev, and T. D. Petes, 2008 High rates of "unselected" aneuploidy and chromosome rearrangements in *tel1 mec1* haploid yeast strains. Genetics **179:** 237–247.

Weinert, T. A., G. L. Kiser, and L. H. Hartwell, 1994 Mitotic checkpoint genes in budding yeast and the dependence of mitosis on DNA replication and repair. Genes Dev. 8: 652–665.

Westmoreland, T. J., J. R. Marks, J. A. Olson Jr., E. M. Thompson, M. A. Resnick *et al.*, 2004 Cell cycle progression in G1 and S phases is *CCR4* dependent following ionizing radiation or replication stress in *Saccharomyces cerevisiae*. Eukaryot. Cell 3: 430–446.

Winzeler, E. A., D. D. Shoemaker, A. Astromoff, H. Liang, K. Anderson *et al.*, 1999 Functional characterization of the *S. cerevisiae* genome by gene deletion and parallel analysis. Science (New York, N.Y.) 285: 901–906.

Wong, K. K., S. Chang, S. R. Weiler, S. Ganesan, J. Chaudhuri *et al.*, 2000 Telomere dysfunction impairs DNA repair and enhances sensitivity to ionizing radiation. Nat. Genet. 26: 85–88.

Woo, S. R., J. E. Park, K. M. Juhn, Y. J. Ju, J. Jeong *et al.*, 2012 Cells with dysfunctional telomeres are susceptible to reactive oxygen species hydrogen peroxide via generation of multichromosomal fusions and chromosomal fragments bearing telomeres. Biochem. Biophys. Res. Commun. 417: 204–210.

Woolstencroft, R. N., T. H. Beilharz, M. A. Cook, T. Preiss, D. Durocher *et al.*, 2006 Ccr4 contributes to tolerance of replication stress through control of *CRT1* mRNA poly(A) tail length. J. Cell Sci. 119: 5178–5192.

Wu, Y., S. Xiao, and X. D. Zhu, 2007 MRE11–RAD50–NBS1 and ATM function as co-mediators of TRF1 in telomere length control. Nat. Struct. Mol. Biol. 14: 832–840.

Wu, Y., P. A. Dimaggio Jr., D. H. Perlman, V. A. Zakian, and B. A. Garcia, 2013 Novel phosphorylation sites in the *S. cerevisiae* Cdc13 protein reveal new targets for telomere length regulation. J. Proteome Res. 12: 316–327.

Zhao, X., A. Chabes, V. Domkin, L. Thelander, and R. Rothstein, 2001 The ribonucleotide reductase inhibitor Sml1 is a new target of the Mec1/Rad53 kinase cascade during growth and in response to DNA damage. EMBO J. 20: 3544–3553.

Zou, L., and S. J. Elledge, 2003 Sensing DNA damage through ATRIP recognition of RPA-ssDNA complexes. Science 300: 1542–1548.

Communicating editor: N. M. Hollingsworth

GENETICS

Supporting Information
http://www.genetics.org/lookup/suppl/doi:10.1534/genetics.113.149849/-/DC1

Novel Connections Between DNA Replication, Telomere Homeostasis, and the DNA Damage Response Revealed by a Genome-Wide Screen for *TEL1/ATM* Interactions in *Saccharomyces cerevisiae*

Brian D. Piening, Dongqing Huang, and Amanda G. Paulovich

DOI: 10.1534/genetics.113.149849

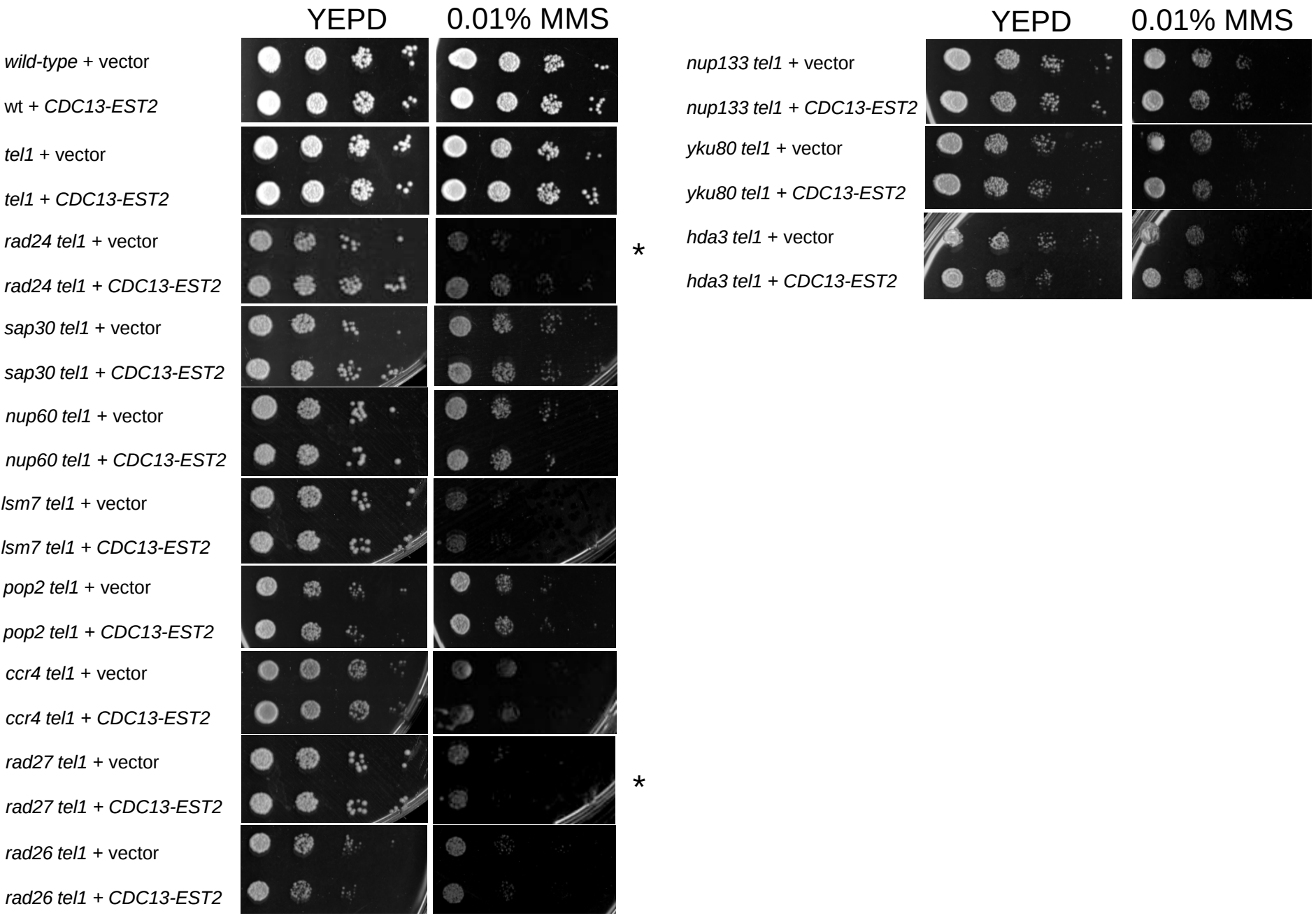

Figure S1 MMS sensitivity with or without the *CDC13-EST2* fusion construct. Strains containing either an empty vector or a *CDC13-EST2* fusion plasmid were cultured in selective media, serially diluted and spotted onto YEPD+/- MMS plates. An asterisk indicates that 0.005% MMS plates were used due to strain sensitivity.